

This is a repository copy of *A mobile ELF4 delivers circadian temperature information from shoots to roots*.

White Rose Research Online URL for this paper:

<https://eprints.whiterose.ac.uk/158324/>

Version: Accepted Version

Article:

Davis, Seth Jon orcid.org/0000-0001-5928-9046, Chen, Wei Wei, Takahashi, Nozomu et al. (6 more authors) (2020) A mobile ELF4 delivers circadian temperature information from shoots to roots. *Nature Plants*. pp. 416-426. ISSN 2055-026X

<https://doi.org/10.1038/s41477-020-0634-2>

Reuse

Items deposited in White Rose Research Online are protected by copyright, with all rights reserved unless indicated otherwise. They may be downloaded and/or printed for private study, or other acts as permitted by national copyright laws. The publisher or other rights holders may allow further reproduction and re-use of the full text version. This is indicated by the licence information on the White Rose Research Online record for the item.

Takedown

If you consider content in White Rose Research Online to be in breach of UK law, please notify us by emailing eprints@whiterose.ac.uk including the URL of the record and the reason for the withdrawal request.

1 **A mobile ELF4 delivers circadian temperature information from shoots to roots**

2

3 Wei Wei Chen^{1*}, Nozomu Takahashi^{1*}, Yoshito Hirata^{2,3}, James Ronald⁴, Silvana Porco⁵, Seth
4 J. Davis^{4,6}, Dmitri A. Nusinow⁷, Steve A. Kay^{5,8} and Paloma Mas^{1,9,†}.

5

6 ¹Centre for Research in Agricultural Genomics (CRAG), CSIC-IRTA-UAB-UB, Campus UAB,
7 Bellaterra, 08193 Barcelona, Spain.

8 ²Mathematics and Informatics Center, The University of Tokyo, 7-3-1 Hongo, Bunkyo-ku,
9 Tokyo 113-8656, Japan.

10 ³Faculty of Engineering, Information and Systems, University of Tsukuba, 1-1-1 Tennodai,
11 Tsukuba, Ibaraki 305-8573, Japan.

12 ⁴Department of Biology, University of York, York, UK.

13 ⁵Keck School of Medicine, University of Southern California, Los Angeles, California 90089,
14 United States.

15 ⁶Key Laboratory of Plant Stress Biology, School of Life Sciences, Henan University,
16 Kaifeng 475004, China.

17 ⁷Donald Danforth Plant Science Center, St. Louis, MO 63132.

18 ⁸Institute of Transformative Bio-Molecules, Nagoya University, Nagoya 464-8601, Japan.

19 ⁹Consejo Superior de Investigaciones Científicas (CSIC), 08028 Barcelona, Spain.

20 *These authors contributed equally the manuscript.

21 †Correspondence to: paloma.mas@cragenomica.es

22

23

24

25

26

27

28

29

30 **Abstract**

31 The circadian clock is synchronized by environmental cues, mostly by light and temperature.
32 Elucidating how the plant circadian clock responds to temperature oscillations is crucial to
33 understand plant responsiveness to the environment. Here we found a prevalent temperature-
34 dependent function of the Arabidopsis clock component ELF4 (EARLY FLOWERING 4) in the
35 root clock. Although the root clock is able to run in the absence of shoots, micrografting assays
36 and mathematical analyses show that ELF4 moves from shoots to regulate rhythms in roots.
37 ELF4 movement does not convey photoperiodic information but trafficking is essential to
38 control the period of the root clock in a temperature-dependent manner. At low temperatures,
39 ELF4 mobility is favored, resulting in a slow-paced root clock while high temperatures decrease
40 movement, leading to a faster clock. Hence, the mobile ELF4 delivers temperature information
41 and establishes a shoot-to-root dialogue that sets the pace of the clock in roots.

42
43

44 **Introduction**

45 Nearly all photosensitive organisms have evolved timing mechanisms or circadian clocks able
46 to synchronize metabolism, physiology and development in anticipation to the 24-hour
47 light/dark cycles¹. In *Arabidopsis thaliana*, the molecular clockwork is based on complex
48 regulatory networks of core clock components that generate rhythms in a myriad of biological
49 outputs^{2, 3}. Appropriate phasing of biological processes relies on clock resetting by light and
50 temperature cues; a mechanism that requires effective changes in the expression and activity of
51 essential clock components⁴. Circadian clocks are also defined by a conserved feature known as
52 temperature compensation⁵. In contrast to the temperature dependency of many
53 physicochemical and biological activities, the circadian clock is able to maintain a constant
54 period over a range of physiological temperatures. By virtue of different transcriptional, post-
55 transcriptional and post-translational mechanisms⁶⁻⁹, the plant circadian system buffers the
56 circadian period length. Therefore, the circadian clock is able to sustain a period close to 24-
57 hours within a physiological range of temperatures. An ample collection of light-related
58 factors¹⁰⁻¹⁴ and clock-associated components^{9, 15, 16} has been shown to directly or indirectly
59 regulate clock temperature compensation in plants.

60

61 Among the Arabidopsis clock components, ELF4 (EARLY FLOWERING 4) was initially
62 identified by its role in photoperiod perception and circadian regulation¹⁷. Structural and
63 functional studies provided a view of the multiple entry points of ELF4 function within the
64 clock¹⁸. ELF4 protein assembles into a tripartite complex (Evening Complex, EC) together with
65 ELF3 and LUX ARRHYTHMO or PHYTOCLOCK1 (LUX/PCL1)^{19, 20}. The complex regulates

66 growth and represses circadian gene expression^{21,22}. ELF4 promotes the nuclear localization of
67 ELF3¹⁹ while LUX directly binds to the promoters of the target genes and thus facilitates the
68 recruitment of ELF4 and ELF3^{20,23}. Loss-of-function mutants of any of the EC components lead
69 to arrhythmia^{17,24-26}. Through multiple interactions with light, clock and photomorphogenesis
70 related factors²⁷, the EC is able to coordinate plant responses to environmental cues including
71 temperature^{15,27-31} although ELF4, ELF3 and LUX also display independent functions from the
72 EC³¹⁻³³.

73

74 Regarding the circadian structure and organization within the plant, it is broadly accepted that
75 every plant cell harbors a circadian oscillator. However, circadian communication or coupling
76 among cells and tissues varies at different parts of the plant³⁴⁻³⁸. For instance, while cotyledon
77 cells present circadian autonomy³⁹, different degrees of cell-to-cell coupling have been reported
78 in leaves⁴⁰⁻⁴², in the vasculature with neighbor mesophyll cells⁴³, in guard cells⁴⁴, in cells at the
79 root tip^{45,46} and within the shoot apex⁴⁷. Long-distance shoot-to-root photosynthetic signaling is
80 also important for clock entrainment in roots⁴⁸ and light piping down the root⁴⁹ contributes to
81 this entrainment. Micrografting assays and shoot excision⁴⁷ suggest the existence of a long-
82 distance mobile circadian signal from shoots to roots. Here we report that ELF4 moves from
83 shoots to control the pace of the root clock in a temperature-dependent manner.

84

85 **Results**

86 **Prevalent function of ELF4 sustaining rhythms in roots**

87 We first approached the investigation of the circadian mobile signal by simultaneously
88 following rhythms in shoots and roots of intact plants⁴⁷. The waveforms of the morning-
89 expressed *CCA1* (*CIRCADIAN CLOCK ASSOCIATED 1*) and *LHY* (*LATE ELONGATED*
90 *HYPOCOTYL*) promoter activities displayed a long period, slightly reduced amplitude and
91 phase delay in roots (Rt) compared to shoots (Sh) (Fig. 1a-b and Extended Data Fig. 1a). The
92 mRNA rhythmic accumulation assayed by Reverse Transcription-Quantitative Polymerase
93 Chain Reaction (RT-QPCR) followed the same trend (Fig. 1c). Similar patterns were observed
94 for the promoter activity of the evening-expressed clock component *TOC1/PRR1* (*TIMING OF*
95 *CAB EXPRESSION1/PSEUDO RESPONSE REGULATOR1*) (Extended Data Fig. 1b-c).
96 Therefore, the clock is fully operative in roots but its overall pace is slower and the phase
97 delayed compared to shoots.

98

99 Under free-running conditions, the circadian clock is unable to properly run in mutant plants of
100 any of the EC components^{17,24-26}. We therefore examined the role of the EC components in the
101 root clock, and in particular, we focused on ELF4. Circadian time course analyses showed that
102 although some very weak oscillations could be appreciated (Extended Data Fig. 1d), the *CCA1*

103 and *LHY* promoter activities and mRNA expression was suppressed in *elf4-1* mutant compared
104 to WT roots (Fig. 1d and Extended Data Fig. 1e-g) following a similar trend to that described in
105 shoots²² (Extended Data Fig. 1h-j). Over-expression of ELF4 (ELF4-ox) lengthened the period
106 of *LHY::LUC* (Fig. 1e and Extended Data Fig. 1k) indicating that increased ELF4 activity in
107 roots makes the clock to run slow. The expression of *PRR9* (*PSEUDO-RESPONSE*
108 *REGULATOR 9*), a previously described direct target of the EC in shoots, was clearly up-
109 regulated in *elf4-1* mutant roots (Fig. 1f) suggesting that the EC also represses *PRR9* in roots.
110 Thus, ELF4 plays an important regulatory function in the root clock: mutation compromises
111 rhythms while over-expression lengthens the circadian period.

112

113 RNA-Seq analyses of WT and *elf4-1* mutant roots provided a genome-wide view of ELF4
114 function in roots (Supplementary Table 1). We found that about 15% of the root genes were
115 significantly mis-regulated by the absence of a functional ELF4, with a similar proportion of up-
116 regulated (1297) and down-regulated (1555) genes (Fig. 1g-h and Extended Data Fig. 2a). The
117 expression of core clock genes was amongst the most significantly mis-regulated (Fig. 1i,
118 Extended Data Fig. 2b-i) with a significant fraction of the mis-regulated genes being controlled
119 by the clock, with phase enrichments during the subjective morning and subjective midday (Fig.
120 1j-k). Functional analyses showed that in addition to the enrichment of genes related to the
121 circadian system and rhythmic processes, genes mis-expressed in *elf4-1* mutant were ascribed to
122 several functional categories including among others responses to stimuli (Supplementary Table
123 1). Consistently, mis-expression of ELF4 affected physiological outputs such as the number of
124 lateral roots (Extended Data Fig. 2j). Together, the results indicate a prevalent function for
125 ELF4 sustaining rhythms in roots.

126

127 **ELF4 moves from shoots to regulate oscillator gene expression in roots**

128 Our previous study showed that a signal from shoots is important for circadian rhythms in roots
129 ⁴⁷. Micrografting assays are a powerful tool to identify the nature of mobile signals. The grafting
130 technique *per se* does not alter the rhythms in roots⁴⁷, as grafted WT scions into WT roots show
131 similar rhythms as non-grafted WT plants (Extended Data Fig. 3a and b). By micrografting
132 different genotypes, we found that grafts of ELF4-ox shoots into *elf4-1* rootstocks [ELF4-
133 ox(Sh)/*elf4-1*(Rt)] (Extended Data Fig. 3c) were particularly efficient in recovering the rhythms
134 in roots (Fig. 2a and Extended Data Fig. 3d). The results are noteworthy as *CCA1::LUC*
135 rhythms are affected in *elf4-1* mutant roots (Fig. 1d). Restoration of the rhythms was reflecting
136 the circadian function exclusively in roots as water instead of luciferin was applied to shoots
137 (ELF4-ox, Sh, H₂O) to avoid luminescence signals leaking from shoots into roots of adjacent
138 wells. Rhythms in roots were also recovered when ELF4-ox scion was grafted into *elf4-2*
139 mutant (Extended Data Fig. 3e) rootstocks (Fig. 2b). To exclude the possibility that the

140 observed results were due to the high over-expression of ELF4-ox plants, we grafted WT shoots
141 into *elf4-1* roots. Although the recovery of the rhythms was not as robust as with ELF4-ox
142 grafts, a rhythmic pattern was observed in roots (Fig. 2c). Thus, ELF4 mRNA or protein are
143 able to move from shoots to roots. This notion was reinforced by the results showing the
144 rhythmic recovery of *elf4-1* rootstocks grafted with ELF4 Minigene (E4MG) scion (Fig. 2d and
145 Extended Data Fig. 3f). These results rule out the possibility that the recovery of the rhythms
146 was just due to the high over-expression of ELF4-ox scion. The influence of shoots as a driving
147 rhythmic force of *elf4-1* rootstocks was also mathematically analyzed with recurrence plots
148 obtained by delay coordinates of the grafting time series. The waveforms of the driving
149 rhythmic force reconstructed from the driven system and their autocorrelation analyses showed
150 a strong periodicity after grafting (Extended Data Fig. 4a-h). In analyses with 10000 randomly
151 shuffled surrogates using as null hypothesis of no serial dependence, we obtained before
152 grafting a p-value of 0.2341 (black dash line) (Extended Data Fig. 4f) and 0.0004 (gray dash
153 line) after grafting (Extended Data Fig. 4h). The statistics are therefore consistent with the
154 notion that rhythms in roots are being forced by a signal from shoots.

155

156 To investigate whether the mRNA could be the mobile signal, we performed RT-QPCR time
157 course analyses of roots from ELF4-ox (Sh)/*elf4-1*(Rt) grafts. Our results showed no detectable
158 amplification of *ELF4* mRNA at any time point analyzed (Fig. 2e), which suggest that *ELF4*
159 mRNA did not move through the graft junctions. To confirm this notion, we injected purified
160 ELF4 protein into *elf4-1* mutant (Extended Data Fig. 5a-c). Injection in shoots was able to
161 restore rhythms in roots (Fig. 2f). The percentage of ELF4-injected plants with recovered
162 rhythms was low (5-8%) but was reproducibly observed in different biological replicates. The
163 fact that rhythms were actually restored (Relative Amplitude Errors, RAE<0.6) is supportive of
164 a mobile ELF4 protein from shoots to roots. Rhythmic recovery was not apparent when purified
165 GFP (GREEN FLUORESCENT PROTEIN) was injected (Fig. 2f). The movement of ELF4
166 protein was further assayed by using shoots of plants over-expressing ELF4 fused to GFP
167 grafted into *elf4-1* mutant roots. Confocal imaging showed that ELF4-GFP fluorescent signals
168 accumulated in the vasculature of *elf4-1* mutant rootstock, across the graft junctions (Fig. 2g-h
169 and Extended Data Fig. 5d-e). Furthermore, Western-blot analyses of roots from ELF4-GFP
170 (Sh)/*elf4-1*(Rt) micrografts showed that ELF4 protein was effectively detected as a band of the
171 expected size (arrows in Fig. 2i) not present in protein extracts of *elf4-1* mutant roots (Fig. 2i).
172 Grafting ELF4-ox fused to three GFPs (ELF4-x3GFP) scion into *elf4-2* mutant rootstock did not
173 lead to an obvious recovery of rhythms (Fig. 2j and Extended Data Fig. 5f) suggesting the
174 requirement of a mobile ELF4 protein. The ELF4-x3GFP is still functional as its over-
175 expression in the *elf4-1* mutant background restored the hypocotyl phenotypes of *elf4-1* mutant
176 (Extended Data Fig. 5g) and repressed *PRR9* gene expression (Extended Data Fig. 5h-i). The

177 functional relevance of ELF4 movement was also verified in *elf4-1*(Sh)/*elf4-1*(Rt) grafts
178 showing the lack of rhythmic recovery in *elf4-1* roots when *elf4-1* was used as scion (Extended
179 Data Fig. 5j-k). Therefore, multiple series of evidence including the ELF4 injection data, the
180 grafting assays showing the recovery of the rhythms, the ELF4-GFP fluorescent signals across
181 the graft junctions, the detection of the ELF4 protein in roots of the grafted plants, the lack of
182 rhythmic recovery in roots of ELF4-x3GFP and in *elf4-1* scion grafts, support the notion that
183 ELF4 protein moves from shoots to regulate rhythms in roots. Other mobile proteins such as FT
184 (FLOWERING LOCUS T), and HY5 (LONG HYPOCOTYL 5) share some features with ELF4
185 protein in terms of low molecular weight and high isoelectric point (Fig. 2k).

186

187 **Blocking ELF4 movement by shoot excision alters circadian rhythms in roots**

188 We next attempted to unveil the function of the mobile ELF4 by blocking ELF4 movement
189 through shoot excision. Analyses of the rhythms showed that excised roots sustained robust
190 oscillations (Extended Data Fig. 6a-b) confirming that the root clock is able to run in the
191 absence of shoots. However, comparison of intact versus excised roots uncovered a shorter
192 period in excised roots (Extended Data Fig. 6c-d). As accumulation of ELF4 results in long
193 periods in shoots²² and roots (Fig. 1e and Extended Data Fig. 1k), it is plausible that blocking
194 ELF4 movement by shoot excision leads to shorter periods in excised roots. If that is the case,
195 blocking ELF4 movement should also affect ELF4 target gene expression in excised roots.
196 Time course analyses by RT-QPCR revealed that the expression of *PRR9* and *PRR7* was up-
197 regulated in excised roots compared to intact roots (Extended Data Fig. 6e-f), which suggest
198 that in the absence of ELF4 movement from shoots, repression of these genes is alleviated in
199 roots. The use of ELF4-ox intact roots confirmed that *PRR9* and *PRR7* are targets of ELF4 as
200 their expression was clearly down-regulated in intact ELF4-ox roots compared to WT intact
201 roots (Extended Data Fig. 6g-h). Furthermore, ELF4-ox excised roots still showed repression of
202 target gene expression (Extended Data Fig. 6i-j) suggesting that excision *per se* is not
203 responsible for the up-regulation observed in WT excised roots.

204

205 To further uncover the function of ELF4 movement, we performed RNA-Seq analyses of WT
206 intact versus excised roots. Our results showed that as expected, a significant fraction of genes
207 was affected by excision (Supplementary Table 2). Comparative analyses of *elf4-1* intact roots
208 with WT excised roots allowed us to discern the effects due to excision from those due to the
209 lack of ELF4 movement (Extended Data Fig. 7). Indeed, we focused on the differentially
210 expressed genes (DEGs) present in both excised WT and intact *elf4-1* roots. As *elf4-1* mutant
211 roots are intact, the overlapping DEGs are not affected by excision *per se* but rather by the lack
212 of ELF4 movement from shoots, which is shared by *elf4-1* intact roots and WT excised roots.

213 Our comparative analyses of both datasets revealed that 67% of the DEGs in *elf4-1* intact roots
214 are also differentially expressed in WT excised roots (Supplementary Table 3) (Extended Data
215 Fig. 7). The proportion of overlapped DEGs (67%) is highly significant (P-value < 0.0001, chi-
216 square test for equality of proportions) as compared to the proportion of overlapping genes
217 (26%) using a random gene list. The overlap is noteworthy due to the different genotypes (*elf4-1*
218 *l* mutant versus WT) and most importantly, the different conditions (intact versus excised). As
219 WT excised roots and *elf4-1* intact roots share the lack of ELF4 movement from shoots, the
220 overlapping DEGs provides a hint about genes that directly or indirectly require ELF4
221 movement for proper expression in roots. Consistently, the overlap of DEGs included nearly all
222 of the core oscillator genes (Supplementary Table 3 and Extended Data Fig. 6k). A significant
223 fraction of overlapped DEGs also circadianly oscillated with phase enrichments during the
224 subjective morning and subjective midday (Extended Data Fig. 6l). Therefore, ELF4 movement
225 appears to be important for a fully functional clock in roots.

226

227 **Mobile ELF4 does not regulate the photoperiodic-dependent phase in roots**

228 In aerial tissues, the circadian clock controls the photoperiodic regulation of growth and
229 development⁵⁰. To determine whether ELF4 movement is important to deliver photoperiodic
230 information, we analyzed rhythms under short day (ShD) and long day (LgD) conditions. In
231 roots, *PRR9::LUC* waveforms displayed a subtle phase delay under LgD compared to ShD (Fig.
232 3a) following a similar trend to that observed in shoots (Fig. 3b). Time course analyses by
233 Western-blot of roots of ELF4 Minigene plants²⁰ confirmed the phase delay of ELF4 protein
234 accumulation under LgD compared to ShD (Fig. 3c-d). We reasoned that if ELF4 movement is
235 correlated with the photoperiodic-dependent phase delay, then excision of shoots might affect
236 the phase shift in roots. In agreement with the oscillations in promoter activity (Extended Data
237 Fig. 6c-d), the phase of ELF4 protein accumulation was advanced following excision under both
238 LgD and ShD (Extended Data Fig. 8a-d). Interestingly, under LgD conditions, excision
239 rendered a similar pattern of ELF4 accumulation than in intact roots under ShD (Fig. 3e-f).
240 Therefore, excision abolished the phase delay observed in intact root under LgD (compare Fig.
241 3c-d with Fig. 3e-f). The results suggest that the photoperiodic-dependent phase shift in roots is
242 hampered by blocking ELF4 movement. However, excised roots still showed the phase delay
243 under LgD compared to excised roots under ShD (Extended Data Fig. 8e-f). Furthermore,
244 analyses of rhythms under LgD conditions showed that plants mis-expressing ELF4 (ELF4-ox
245 and *elf4-1* mutant) displayed very similar rhythms to WT both in shoots and roots (Fig. 3g-h)
246 suggesting that ELF4 function is not essential to sustain rhythms under entraining conditions.
247 Together, the results suggest that blocking ELF4 movement by excision advances the phase of
248 the root clock but the mobile ELF4 does not directly regulate the photoperiodic-dependent
249 phase shift in roots.

250

251 **ELF4 movement contributes to the temperature-dependent changes in circadian period of**
252 **the root clock**

253 As the EC also coordinates temperature responses, we examined whether a mobile ELF4 can
254 convey temperature information from shoots to roots. To that end, we first examined the effect
255 of different temperatures (28°C, 18°C and 12°C) on circadian rhythms in roots. We found that
256 *LHY::LUC* circadian period length was shorter at high than at low temperatures (Extended Data
257 Fig. 9a-b). Shortening of period length at increasing temperature was also observed for other
258 circadian reporter lines (Extended Data Fig. 9c-f) indicating that at this developmental stage and
259 under our experimental conditions, the circadian clock in roots is not able to perfectly sustain
260 circadian period length within a range of temperatures.

261

262 As ELF4 accumulation lengthens period length, we next examined the possible contribution of
263 ELF4 to the long period phenotype at low temperatures. Changes in period length could be
264 mediated by increased ELF4 activity and/or by the increased protein movement from shoots to
265 roots. To examine these possibilities, we compared the effects of blocking ELF4 movement by
266 excision at low and high temperatures. Essentially, if the long period in roots at 12°C is
267 independent of movement but results from the increased activity of ELF4, blocking movement
268 from shoots by excision should not have a major effect on period length. However, if ELF4
269 movement contributes to the period regulation, abolishing ELF4 traffic should lead to an
270 observable and differential effect on period length at different temperatures.

271

272 Our results showed that excision shortened the period length in WT roots and this effect was
273 significant at 12°C as compared to the minor effect at 28°C (Extended Data Fig. 10a-d).
274 Therefore, blocking ELF4 movement by excision shortens the long period of WT roots at 12°C.
275 Analyses of other circadian reporter lines and at 18°C also showed that excision shortened
276 period length compared to intact roots (Extended Data Fig. 10e-f). The results suggest a
277 temperature-dependent control of ELF4 movement that regulates period length in roots. To
278 further verify this notion, we examined rhythmic recovery in grafts of ELF4-ox scion into *elf4-1*
279 rootstock at low and high temperatures. Our results showed an evident rhythmic recovery at
280 12°C but not at 28°C (Fig. 4a-b). Furthermore, grafts of E4MG scion into *elf4-1* rootstock also
281 efficiently recovered rhythms at 12°C but not at 28°C (Fig. 4c-d). ELF4 is still able to delay the
282 phase and lengthen the period at 28°C (Fig. 4e and Extended Data Fig. 10g) suggesting that
283 movement rather than changes in activity are responsible for the observed effects. ELF4 protein
284 accumulation in roots of ELF4-ox scion into *elf4-1* rootstock was higher at 12°C than at 28°C
285 (Figure 4f and Extended Data Fig. 10h-i) but ELF4 (E4MG) protein accumulation in shoots is

286 similar at different temperatures³¹ (Extended Data Fig. 10j). Therefore, ELF4 movement rather
287 than protein accumulation or activity appears to be regulated by temperature, contributing to the
288 temperature-dependent control of circadian period in roots.

289

290 Altogether, we propose a model by which mobile ELF4 (mbE4) from shoots to roots defines a
291 pool of active ELF4 protein that is competent to repress target circadian gene expression in
292 roots. ELF4 trafficking is favored at low temperatures, which results in a slow-paced clock (Fig.
293 4g) while high temperatures decrease the movement, leading to a fast root clock (Fig. 4h). The
294 temperature-dependent movement of ELF4 allows a shoot-to-root dialogue that controls the
295 pace of the clock and provides a mechanism by which temperature cues from shoots set the
296 circadian period length in roots.

297

298 **Discussion**

299 The simultaneous examination of rhythms in shoots and roots of single individual plants shows
300 that the promoter activities and mRNA accumulation of clock genes in roots display a longer
301 period and delayed phase compared to shoots. The trend was observed for morning- and
302 evening-expressed key oscillator genes suggesting that the overall circadian system in roots is
303 not as precise as in other parts of the plant (e.g. the shoot apex)⁴⁷. Despite the long period, the
304 rhythms persist in roots for several days under LL, which is reminiscent of a fully functional
305 clock. The lack of precision might provide circadian flexibility for rapid adjustments and
306 improved responses in roots. Previous studies have reported spatial waves of clock gene
307 expression with and within organs^{40, 42, 45} that might be due to differences in period length and
308 variable local coupling.

309

310 The EC directly represses *PRR9* and *PRR7* expression^{19, 23, 29, 51, 52} and indirectly promotes the
311 expression of the morning-expressed oscillator genes *CCA1* and *LHY*⁵¹⁻⁵⁴. Our analyses with
312 *elf4-1* mutant and ELF4-ox plants demonstrate that ELF4 function in roots is also important for
313 proper repression of *PRR9* and *PRR7* and activation of *CCA1* and *LHY*. ELF4 regulatory
314 function in roots appears to be similar to that previously described for the EC using whole
315 plants. Over-expression of ELF4 lengthens the period of the root clock suggesting that ELF4
316 slows down the circadian period in roots as in shoots²². The fact that accumulation of ELF4
317 lengthens the period agrees with the results showing that blocking movement by shoot excision
318 shortens the period. RNA-Seq analyses revealed that not only the expression of oscillator genes
319 is affected in *elf4-1* roots but also a battery of genes involved in other pathways including
320 responses to stimuli. These pathways are also consistent with the EC function in responses to
321 environmental cues⁵⁵. The mis-regulated genes in *elf4-1* roots might be direct targets of ELF4

322 and/or indirect outputs of the clock in roots. One of these outputs might be lateral root
323 emergence as the number of lateral roots is affected in *elf4-1* and ELF4-ox compared to WT.
324 Future studies are necessary to uncover the molecular and cellular mechanisms by which ELF4
325 regulates the number of lateral roots in Arabidopsis.

326

327 Micrografts of ELF4-ox scion into *elf4-1* or *elf4-2* rootstocks allow a remarkable recovery of
328 rhythms that is not observed when seedlings expressing ELF4 protein fused to 3 GFPs in
329 tandem is used as scion. These results suggest that ELF4 movement is indeed important for the
330 rhythmic recovery. Fluorescent signals accumulating in the vasculature of *elf4-1* mutant
331 rootstock grafted with ELF4-GFP scion and the detection of the ELF4 protein in roots of the
332 micrografted plants also suggest that ELF4 moves from shoots to roots. This conclusion is
333 complemented with the grafting assays of *elf4-1*(Sh)/*elf4-1*(Rt) showing the lack of rhythmic
334 recovery in roots, and with the assays of ELF4 protein injection in shoots and the subsequent
335 rhythmic recovery in roots. Micrografts of E4MG and WT plants are also able to recover the
336 rhythms of the *elf4-1* mutant roots, which indicate that the effects are not due to the over-
337 accumulation of ELF4-ox and suggest that the amount of mobile ELF4 that is required to
338 regulate the rhythms is probably not very high. Our experiments adding water to the scion or
339 using WT scion without LUC reporter exclude the possibility that rhythms in grafted roots are
340 due to leakage for the adjacent well containing the shoot. The fact that ELF4 protein shows
341 similar properties in terms of length, molecular weight and isoelectric point to other mobile
342 proteins⁵⁶⁻⁵⁹ also support the notion of ELF4 movement. We postulate that following movement,
343 the complex regulatory feedback loops at the core of the oscillator will be reset to control the
344 pace of the clock. Further experiments at different developmental stages and various growing
345 conditions (e.g. light and temperature) will be required to confirm whether the long distance
346 movement of ELF4 contributes or not to the spatial waves of clock gene expression observed in
347 roots⁴².

348

349 Excision blocks ELF4 movement from shoots and consequently, we observe that oscillator gene
350 expression and other output genes are affected in WT excised roots. Previous studies have also
351 used excision to define properties of the circadian function in roots⁴². Although many genes are
352 affected by excision, it is noteworthy that 67% of the genes mis-regulated in *elf4-1* intact roots
353 are also mis-expressed in WT excised roots. Both conditions share the lack of ELF4 movement,
354 which suggest that the overlapped DEGs are due to the lack of a mobile ELF4 (note that the
355 RNA-Seq studies with *elf4-1* mutant were performed with intact roots). The phase shifts
356 observed following excision prompted us to examine whether ELF4 movement contributed to
357 the photoperiodic-dependent phase shift. However, excised roots still sustained the phase delay
358 under LgD suggesting that other factors are responsible for this regulation. Light piping down

359 the root⁴⁹ might be also important for synchronization. Regardless the mechanism, it is able to
360 overcome the mis-expression of ELF4 in shoots and roots as ELF4-ox and *elf4-1* mutant plants
361 displayed similar rhythms to WT. Clear alteration of circadian expression under LL but not
362 under entraining conditions has been reported for other clock mutants and over-expressing
363 plants⁶⁰.

364

365 The EC activity is down-regulated at high temperatures in whole seedlings^{29,31}. Shoot excision
366 shortened the period, suggesting that ELF4 movement is important in the control of circadian
367 period length. Period shortening is more significant at low than at high temperatures confirming
368 that ELF4 movement might be favored at low temperatures. The temperature-dependent control
369 of ELF4 movement is also supported by the increased accumulation ELF4 protein in grafted
370 roots at 12°C compared to 28°C. As ELF4 accumulation results in long period, the increased
371 movement leads to a clock that runs slower at low than at high temperatures. It would be
372 interesting to elucidate whether period sensitivity to temperature might provide an advantage for
373 optimal root responsiveness to temperature variations.

374

375 **Methods**

376 **Plant material, growth conditions, constructs and physiological assays**

377 *Arabidopsis thaliana* seedlings were stratified at 4°C in the dark for 2-3 days on Murashige and
378 Skoog (MS) agar medium with 3% of sucrose (MS3). Plates were transferred to chambers with
379 light- and temperature-controlled conditions with 25-50 $\mu\text{mol}\cdot\text{quanta}\cdot\text{m}^{-2}\cdot\text{s}^{-1}$ of cool white
380 fluorescent light. Seedlings were synchronized under Light:Dark cycles, LD (12h light: 12h
381 dark) at 22°C. For experiments with different temperatures, seedlings were analyzed under
382 constant light conditions at 12°C, 18°C, 22°C or 28°C following synchronization under LD (12h
383 light: 12h dark) at 22°C. For experiments with different photoperiods, seedlings were grown
384 under short days (ShD, 8h light: 16h dark) or long days (LgD, 16h light: 8h dark). Reporter
385 lines *CCA1::LUC*⁶¹, *LHY::LUC*¹⁹, *PRR9::LUC*⁶², *TOC1::LUC*⁶ and *elf4-1*¹⁷, *elf4-2*²⁷, ELF4
386 Minigene²⁰ and ELF4-GFP-ox^{19,20} plants were described elsewhere. The ELF4 construct fused
387 to three Green Fluorescent Proteins (GFPs) in tandem was generated by PCR-mediated
388 amplification of the *ELF4* coding sequence and subsequent subcloning into the PGWB514
389 gateway vector^{63,64}. The resulting plasmid was digested with PacI and SacI restriction enzymes
390 and ligated with the 3 GFPs insert from the pBS-x3GFP vector (Addgene). The construct was
391 transformed into *elf4-1* mutant plants. Plants were transformed using *Agrobacterium*
392 *tumefaciens* (GV2260)-mediated DNA transfer⁶⁵. For in vitro protein injection assays, the ELF4
393 coding sequence was subcloned into the pET MBP_1a vector (Novagen) after removing the
394 GFP by Nco I and Xho I restriction enzyme digestion.

395

396 For lateral root analyses, WT, *elf4-1* and ELF4-ox seeds were surface-sterilized and plated onto
397 MS medium supplemented with 0.25% w/v sucrose and 1.5% agar. The top quarter of the agar
398 was removed and seeds pipetted evenly along this line. Plants were then grown vertically for 12
399 days before lateral roots were measured. Lateral roots were manually counted using a Nikon
400 SMZ800 dissecting microscope. Statistical analysis was completed using R (version 3.6), within
401 the R studio software package (version 1.1.4). For hypocotyl elongation measurements, WT,
402 *elf4-1*, ELF4-GFP-ox and ELF4-3xGFP-ox seeds transformed into the *elf4-1* mutant
403 background were stratified on MS3 medium in the dark for 4 days at 4°C, exposed to white light
404 ($40 \mu\text{mol}\cdot\text{quanta}\cdot\text{m}^{-2}\cdot\text{s}^{-1}$) for 6 h and maintained in the dark (22°C) for 18 h before transferring
405 to chambers under Short-Day conditions (8h light:16h dark). Hypocotyl length was measured
406 using the ImageJ software (version 1.48v) (<https://imagej.nih.gov/ij/>) at 7 days after
407 stratification. Each experiment was repeated at least twice using 20-50 seedlings per genotype.
408 Statistical analyses were performed using the GraphPad Prism software (version 5.01;
409 GraphPad Software, Inc) using two-tailed t-tests with 95% of confidence.

410

411 **In vivo luminescence assays**

412 In vivo luminescence assays were performed as previously described⁴⁷. Briefly, 7-15 day-old
413 seedlings synchronized under LD cycles at 22°C were transferred to 96-well plates and released
414 into the different conditions as specific for each experiment. Analyses were performed with a
415 LB960 luminometer (Berthold Technologies) using the Microwin software (Version 4.41;
416 Mikrotek Laborsysteme). The period, phase and amplitude were estimated using the Fast
417 Fourier Transform–Non-Linear Least Squares (FFT–NLLS) suite⁶⁶ using the Biological
418 Rhythms Analysis Software System (version 3.0; BRASS, <http://www.amillar.org>). For the
419 simultaneous analysis of rhythms of shoots and roots from the same plant, the connection
420 between the two adjacent wells of the 96-well plates was serrated. Seedlings were then
421 horizontally positioned so the shoot was placed in one well and the roots in the contiguous well.
422 For excision analyses, roots were excised from shoots and placed into the 96-well plates for
423 luminescence analyses. Data from samples that appeared damaged or contaminated were
424 excluded from the analysis. For analyses of grafted samples, water instead of luciferin was
425 applied to the wells containing shoots to avoid possible leaking signals from shoots to roots as
426 specified. At least two biological replicates were performed per experiment, with measurements
427 taken from distinct samples grown and processed at different times. Each biological replicate
428 included 6 to 12 independent seedlings per condition and/or genotype. Statistical analyses were
429 performed using the GraphPad Prism software (version 5.01; GraphPad Software, Inc) using
430 two-tailed t-tests with 95% of confidence.

431

432

433 **Protein purification and injection analyses**

434 *E. coli* cells (BL21, Dh5 α) were transformed and grown in LB medium (Tryptone 10 g/L, yeast
435 extract 5 g/L, NaCl 10 g/L pH 7.5) until OD600 values of 0.8-1.0. Isopropyl β -D-1-
436 thiogalactopyranoside (IPTG)-mediated induction of MBP-ELF4 and MBP-GFP was performed
437 at 28°C for 6 h. Bacteria resuspended in lysis buffer (50mM Tris-HCl, pH7-8, 5% glycerol,
438 50mM NaCl) were lysed by sonication for 2-3 minutes (30s on, 30s off, high intensity) using a
439 sonicator (Bioruptor, Diagenode). Recombinant proteins were purified using gravity flow
440 columns with amylose resin (New England Biolabs). MBP cleavage was performed by
441 incubation in cleavage buffer (50 mM Trizma-HCl, pH 8.0, 0.5 mM EDTA, and 1 mM DTT)
442 for 2 hours at 30°C with native Tobacco Etch Virus (TEV) protease (Sigma-Aldrich). The
443 purified recombinant proteins were concentrated using Amicon centrifugal filters following the
444 manufacturer recommendations (Millipore). Protein yield was estimated by measuring
445 absorbance at 595 nm using a spectrophotometer (UV-2600, SHIMADZU). Proteins were also
446 examined by Coomassie-Brilliant Blue staining of polyacrylamide gels to confirm protein size
447 and integrity. Purified ELF4 was injected into leaves of 10-day old *elf4-1* mutant seedlings
448 harboring the *LHY::LUC* reporter line. Similar concentration of GFP protein was also injected
449 as a negative control. Rhythms were subsequently examined in a LB960 luminometer (Berthold
450 Technologies) as described above.

451

452 **Time course analyses of gene expression by RT-qPCR**

453 Seedlings were synchronized under LD cycles in MS3 medium plates for 12-14 days and
454 subsequently transferred to LL. Shoots and roots from intact plants were taken every 4 hour
455 over the circadian cycle. For excised roots, shoots and roots were carefully separated with a
456 sterile razor blade and the excised roots were deposited on MS3 agar medium plates for 2 or 3
457 days as specified. RNA was purified using a Maxwell RSC Plant RNA kit following the
458 manufacturer's recommendations (Promega). Single-stranded cDNA was synthesized using
459 iScript Reverse Transcription Supermix for RT-qPCR (Bio-Rad). qPCR analyses were
460 performed with cDNAs diluted 50-fold with nuclease-free water using Brilliant III Ultra-Fast
461 SYBR Green qPCR Master Mix (Agilent) with a 96-well CFX96 Touch Real-Time PCR
462 detection system (Bio-RAD CFX96 Manager version 3.1, Bio-Rad). Each sample was run in
463 technical triplicates. The expression of *PP2AA3* (*PROTEIN PHOSPHATASE 2A SUBUNIT A3*,
464 AT1G13320) or *MON1* (*MONENSIN SENSITIVITY1*, AT2G28390)⁶⁷ was used as a control.
465 Crossing point (Cp) calculation was used for quantification using the Absolute Quantification
466 analysis by the 2nd Derivative Maximum method. At least two biological replicates were

467 performed, with measurements taken from distinct samples grown and processed at different
468 times.

469

470 **RNA-Seq analyses**

471 Roots from 14-day old intact WT, *elf4-1* mutant and excised WT plants synchronized under LD
472 cycles in MS3 medium plates were transferred to LL conditions for 3 days. Roots were excised
473 just before transferring to LL. Samples were collected at the fourth day under LL at circadian
474 time 75 (CT75). Total RNA was isolated using a Maxwell RSC Plant RNA kit. RNA
475 sequencing was performed by IGATech (Italy). About 1-2 µg of high quality RNA (R.I.N. >7)
476 was used for library preparation with a TruSeq Stranded mRNA Sample Prep kit' (Illumina, San
477 Diego, CA). Poly-A mRNA was fragmented for 3 minutes at 94°C. Purification was performed
478 with 0.8x Agencourt AMPure XP beads. Both RNA samples and final libraries were quantified
479 using the Qubit 2.0 Fluorometer (Invitrogen, Carlsbad, CA). Quality was tested using the
480 Agilent 2100 Bioanalyzer RNA Nano assay (Agilent technologies, Santa Clara, CA). Libraries
481 were then processed with Illumina cBot for cluster generation on the flowcell, following the
482 manufacturer's instructions and sequenced on paired-end mode at the multiplexing level
483 requested on HiSeq2500 (Illumina, San Diego, CA). The CASAVA (1.8.2 version) of the
484 Illumina pipeline was used to process raw data for both format conversion and de-multiplexing.

485

486 Sequence analysis was performed using the A.I.R. software (version 1.0)
487 (<https://transcriptomics.sequentiabiotech.com/>) developed by Sequentia Biotech. Briefly, raw
488 sequence files were first subjected to quality control analysis by using FastQC (v0.10.1) before
489 trimming and removal of adapters with BBDuk (<https://jgi.doe.gov/data-and-tools/bbtools/>).
490 Reads were then mapped against the *Arabidopsis thaliana* genome (TAIR10 Genome Release,
491 <ftp://ftp.arabidopsis.org/>) with STAR (version 2.6)⁶⁸. FeatureCounts (version 1.6.1)⁶⁹ was then
492 used to obtain raw expression counts for each annotated gene. The differential expression
493 analysis was conducted with edgeR (version 3.18.1)⁷⁰, using the TMM normalization method.
494 FPKM were obtained with edgeR.

495

496 The Integrative Genomics Viewer (IGV, version 2.4.13)
497 (<https://software.broadinstitute.org/software/igv/>) was used to visualize the data^{74, 75}. The
498 circadian phases were analyzed using the publicly available Gene Phase Analysis Tool
499 "PHASER" of the DIURNAL database (<http://diurnal.mocklerlab.org/>)^{76, 77}. Phase over-
500 representation is calculated as the number of genes with a given phase divided by the total
501 number of genes over the number of genes called rhythmic and divided by the total number of
502 genes in the dataset. Functional categories of the DEG were obtained using the web tool
503 "BIOMAPS"(VirtualPlant, version 1.3)⁷⁸, which renders over-represented and significant

504 functional terms (Gene Ontology or MIPS) as compared to the frequency of the term in the
505 whole genome.

506

507 **Western-blot assays**

508 Approximately 50-100 mgs of roots from plants grown under the specified photoperiodic
509 condition were sampled every four hours over a 24-hour cycle. Samples were rapidly frozen
510 with liquid nitrogen and grounded with stainless steel beads (Millipore) in a tissue lyser
511 (QIAGEN, TissueLyser II). Tissue was subsequently resuspended in Protein Extraction Buffer
512 (PEB) containing 50 mM Tris-HCl pH 7.5, 150 mM NaCl, 0.5% NP40, 1 mM EDTA, and
513 protease inhibitors cocktail (1:100) and PMSF (1:1000). Protein extracts were centrifuged at
514 4 °C, measured for protein concentration using Bradford reagent (Bio-Rad) and normalized to 2
515 mg/ml in 4 x SDS loading buffer (250 mM Tris-HCl, pH 6.8, 8% SDS, 0.08% bromophenol
516 blue, 40% glycerol). Samples were run on a 12% gel and analyzed by immunoblotting, fixed 30
517 min with 0.4% Glutaraldehyde solution (Sigma-Aldrich) and detected with an anti-HA antibody
518 (Roche) (1:2000 dilution) and a goat anti-rat horse peroxidase conjugated secondary antibody
519 (Sigma-Aldrich) (1:4000 dilution). For analyses of the grafted plants, roots from plants
520 synchronized under LD cycles were subsequently transferred to LL for 3 days at 12°C, 22°C or
521 28°C. Samples were collected at CT81, rapidly frozen with liquid nitrogen and grounded with
522 stainless steel beads (Millipore) in a tissue lyser (QIAGEN, TissueLyser II). Powder extracts
523 were subsequently resuspended in Protein Extraction Buffer (PEB) containing 50 mM Tris-HCl
524 pH 7.5, 150 mM NaCl, 0.5% NP40, 1 mM EDTA, and protease inhibitors cocktail (1:100),
525 PMSF (1:1000), and MG132 (100uM). Protein extracts were centrifuged at 4 °C, measured for
526 protein concentration using Bradford reagent (Bio-Rad) and normalized to 2 µg/µl in 4 x SDS
527 loading buffer (250 mM Tris-HCl, pH 6.8, 8% SDS, 0.08% bromophenol blue, 40% glycerol
528 and 5 mM β-mercaptoethanol). For detection of ELF4 protein fused to GFP, samples were run
529 on a 10% gel and was detected using an anti-GFP antibody (ab290, Abcam) (1:5000) and Goat
530 anti-Rabbit IgG (H+L) Secondary Antibody, HRP (31460, Lot: OG188649, Thermo Fisher
531 Scientific) (1:5000 dilution). For detection of ELF4 protein fused to HA (ELF4 Minigene) in
532 shoots, samples were resuspended in Protein Extraction Buffer (PEB) containing 50mM
533 TrisHCl pH7.5, 150mM NaCl, 0.5% NP40, 1mM EDTA, protease inhibitors and proteasome
534 inhibitor (MG132, 100uM). Protein extracts in 4× SDS loading buffer (250 mM Tris-HCl, pH
535 6.8, 8% SDS, 0.08% bromophenol blue, 40% glycerol, 5 mM β-mercaptoethanol) were run on a
536 12% gel and analyzed by immunoblotting, fixed 30 min with 0.4% Glutaraldehyde solution
537 (Sigma-Aldrich) and detected with an Anti-HA antibody High Affinity from rat IgG1
538 (11867423001, Sigma-Aldrich) (1:2000) and a goat anti-rat horse peroxidase conjugated
539 secondary antibody (A9037, Sigma-Aldrich) (1:4000). The Image Lab software (version 5.2.1;
540 Bio-Rad) was used to image the Western-blot. Membranes were stained with a Ponceau S

541 solution following the manufacturer recommendations (Sigma). Proteins were also run on a
542 10% SDS-PAGE gel and stained with Coomassie-Brilliant Blue. At least two biological
543 replicates were performed per experiment and/or condition, with measurements taken from
544 distinct samples grown and processed at different times.

545

546 **Micrografting assays**

547 Micrografting was performed essentially as previously described⁴⁷. Data from unsuccessful
548 grafted seedlings that failed to properly join together or grafts that were insufficiently clear to be
549 successful were discarded. Approximately 100-150 grafting events were performed for every
550 combination of grafts. The percentage of successfully micrografted plants was about 30-50 %
551 (possibly higher but only the clearly successful grafted plants were taken into account). From
552 the successfully grafted plants, 30-60 % showed different degrees of recovered rhythms. For in
553 vivo luminescence assays, shoots and roots of grafted plants were simultaneously examined
554 using the protocol described above. Water instead of luciferin was added to the wells containing
555 shoots to exclude the possibility that recovery of rhythms in roots were due to leaking signals
556 from shoots. As specified, some grafted shoots contained no reporter fused to luciferase.

557

558 **Reconstruction of driving forces by recurrence plots**

559 Common driving forces were estimated following a several-step procedure. Suppose that we
560 have the number K of simultaneous time series measurements $\{s_i(t) | i = 1, 2, \dots, K, t =$
561 $1, 2, \dots, T\}$. First, we took time differences $\tilde{s}_i(t) = s_i(t + 1) - s_i(t)$ ($i = 1, 2, \dots, K, t =$
562 $1, 2, \dots, T - 1$) of consecutive measurements and remove trends. Second, we used delay
563 coordinates^{79, 80} $\vec{\tilde{s}}_i(t) = [\tilde{s}_i(t), \tilde{s}_i(t + 1), \tilde{s}_i(t + 2), \tilde{s}_i(t + 3), \tilde{s}_i(t + 4)]$ of 5 dimensional space
564 ($i = 1, 2, \dots, K, t = 1, 2, \dots, T - 4$) to obtain a recurrence plot⁸¹. A recurrence plot is a two-
565 dimensional figure proposed originally for visualizing time series data. Both axes are the same
566 time axis. If the Euclidean distance $\|\vec{\tilde{s}}_i(t_1) - \vec{\tilde{s}}_i(t_2)\| < \varepsilon_i$, where ε_i is a threshold and $t_1, t_2 \in$
567 $\{1, 2, \dots, T - 4\}$, then we plot a point at (t_1, t_2) . We denote this as $R_i(t_1, t_2) = 1$. Otherwise, we
568 do not plot a point at (t_1, t_2) . We denote this state as $R_i(t_1, t_2) = 0$. We controlled the value of
569 the threshold ε_i for each component $i \in \{1, 2, \dots, K\}$ so that 5% points, except for the central
570 diagonal line, have points plotted. Third, we took the union for the recurrence plots to infer the
571 recurrence plot of the common driving force⁸². Namely we declare $R(t_1, t_2) = 1$ if we have
572 $R_i(t_1, t_2) = 1$ for at least one of $i \in \{1, 2, \dots, K\}$. Otherwise, we have $R(t_1, t_2) = 0$. In each of
573 the original recurrence plots, points are plotted where the driving force and the driven system
574 are both similar. By taking their union, we can extract pairs of times where only the driving
575 force is similar. Fourth, we applied the assumption of continuity and supplied the points at
576 $(t, t+1)$ and $(t+1, t)$ for each i ⁸³. Namely, we forcefully declare $R(t, t + 1) = R(t + 1, t) = 1$ for

577 $t = 1, 2, \dots, T - 5$. Fifth, we applied the method described⁸² to convert the recurrence plot of the
578 common driving force into time series. Here we describe the detail for this step: (i) we construct
579 a network where each node correspond to a time point and we connect two nodes t_1 and t_2 if
580 $R(t_1, t_2) = 1$; (ii) we assign a distance for each edge as $1 - \frac{\#\{k=1,2,\dots,T-4|R(k,t_1)=1 \text{ and } R(k,t_2)=1\}}{\#\{k=1,2,\dots,T-4|R(k,t_1)=1 \text{ or } R(k,t_2)=1\}}$;
581 (iii) we obtain the shortest distance for each pair of nodes on this graph (this process
582 approximates the geodesic distance between two time points); (iv) we apply the multi-
583 dimensional scaling to convert the distance matrix to a time series. Namely this fifth step works
584 as the inverse transform of a recurrence plot and we can reproduce a rough shape for the
585 original time series. This fifth step has two mathematical proofs^{84, 85}. Lastly, we extracted the
586 component corresponding to the largest eigenvalue. The periodicity of the reconstructed
587 common driving force $X(t)$ was evaluated using the autocorrelation function and 10000 random
588 shuffle surrogates⁸⁶, for each of which the order of time points is randomly exchanged. Here, the
589 null hypothesis was that there was no serial dependence. The autocorrelation with time
590 difference k is the correlation coefficient between $X(t)$ and $X(t+k)$. Thus, it is close to 1 if $X(t)$
591 and $X(t+k)$ are similar while it is close to 0 if they are not related to each other. If there is a 24h
592 periodicity in the driving force, the autocorrelation with 24h time difference should be a value
593 close to 1.

594 **Confocal imaging**

595 For *in vivo* confocal imaging, the roots of WT and ELF4-ox (fused to GFP) grafted shoots into
596 *elf4-1* mutants were placed on microscope slides (Sigma). Fluorescent signals were imaged with
597 an argon laser (transmissivity: 40%; excitation: 515 nm; emission range: 530–630 nm) in a
598 FV-1000 confocal microscope (Olympus, Tokyo, Japan) using a FV-10-ASW4.2 Viewer
599 Manager software (Olympus) with a 40x/1.3 oil immersion objective. The image sizes were
600 about 640 x 640 (0.497 $\mu\text{m}/\text{pixel}$) and sampling speed of 4 $\mu\text{s}/\text{pixel}$. The results are
601 representative of at least three biological replicates for grafting and about three-four images per
602 grafts.

603

604 **List of primers.** List of primers used for expression analyses, cloning and generation of 3x GFP
605 construct.

| Name | Sequence | Experiment |
|---------------------|----------------------------|---------------------|
| REF1(PP2A_A3)_EXP_F | AAGCGTTGTGGAGAACATGATACG | Expression analysis |
| REF1(PP2A_A3)_EXP_R | TGGAGAGCTTGATTTGCGAAATACCG | Expression analysis |
| MON1_EXP_F | AACTCTATGCAGCATTTGATCCACT | Expression analysis |
| MON1_EXP_R | TGATTGCATATCTTTATCGCCATC | Expression analysis |
| PRR7_EXP_F | AAGTAGTGATGGGAGTGGCG | Expression analysis |
| PRR7_EXP_R | GAGATACCGCTCGTGGACTG | Expression analysis |
| PRR9_EXP_F | ACCAATGAGGGGATTGCTGG | Expression analysis |

| | | |
|-----------------|----------------------------------|---------------------------|
| PRR9_EXP_R | TGCAGCTTCTCTCTGGCTTC | Expression analysis |
| ELF4_EXP_F | GACAATCACCAATCGAGAAT | Expression analysis |
| ELF4_EXP_R | ATGTTTCCGTTGAGTTCTTG | Expression analysis |
| CCA1_EXP_F | TCGAAAGACGGGAAGTGGAAACG | Expression analysis |
| CCA1_EXP_R | GTCGATCTTCATTGGCCATCTCAG | Expression analysis |
| LHY_EXP_F | AAGTCTCCGAAGAGGGTTCGT | Expression analysis |
| LHY_EXP_R | GGCGAAAAGCTTTGAGGCAA | Expression analysis |
| ELF4_CLN_F | CACCATGAAGAGGAACGGCGA | Cloning |
| ELF4_CLN_R | AGCTCTAGTTCCGGCAGCACCA | Cloning |
| MBP-ELF4_CLN_F | CATGCCATGGGCATGAAGAGGAACGGCGAG | Cloning |
| MBP-ELF4_CLN_R | CCGCTCGAGTTAAGCTCTAGTTCCGGCAGCAC | Cloning |
| PacI-pBS3xGFP-F | GGTTAATTAACGCTGGAGGATCCATGTCTA | Generation of pGWB-c3xGFP |
| SacI-pBS3xGFP-R | TCGAGCTCTCTAGAACTAGTGGATCTTTA | Generation of pGWB-c3xGFP |

606

607

608 **Reporting Summary.** Further information on research design is available in the Nature
609 Research Reporting Summary linked to this article.

610

611 **Data availability**

612 Data and materials generated in this study are available without restriction and should be
613 requested to Paloma Mas: paloma.mas@cragenomica.es. NGS data are deposited in NCBI with
614 accession code PRJNA610472 (BioSample accessions SAMN14299292, SAMN14299293,
615 SAMN14299294). Source data are provided for all figures.

616

617 **References**

- 618 1. Zhang, E.E. & Kay, S.A. Clocks not winding down: unravelling circadian networks.
619 *Nat. Rev. Mol. Cell. Biol.* **11**, 764-776 (2010).
- 620 2. Greenham, K. & McClung, C.R. Integrating circadian dynamics with physiological
621 processes in plants. *Nat. Rev. Genet.* **16**, 598-610 (2015).
- 622 3. Nagel, Dawn H. & Kay, Steve A. Complexity in the wiring and regulation of plant
623 circadian networks. *Curr. Biol.* **22**, R648-R657 (2012).
- 624 4. Oakenfull, R.J. & Davis, S.J. Shining a light on the Arabidopsis circadian clock. *Plant*
625 *Cell Environ* **40**, 2571-2585 (2017).
- 626 5. Hogenesch, J.B. & Ueda, H.R. Understanding systems-level properties: timely stories
627 from the study of clocks. *Nature Reviews Genetics* **12**, 407 (2011).
- 628 6. Portolés, S. & Más, P. The functional interplay between protein kinase CK2 and CCA1
629 transcriptional activity is essential for clock temperature compensation in Arabidopsis.
630 *PLoS Genetics* **6**, e1001201 (2010).
- 631 7. Hansen, L.L., van den Burg, H.A. & van Ooijen, G. Sumoylation Contributes to
632 Timekeeping and Temperature Compensation of the Plant Circadian Clock. *J Biol*
633 *Rhythms* **32**, 560-569 (2017).
- 634 8. Marshall, C.M., Tartaglio, V., Duarte, M. & Harmon, F.G. The Arabidopsis *sickle*
635 Mutant Exhibits Altered Circadian Clock Responses to Cool Temperatures and
636 Temperature-Dependent Alternative Splicing. **28**, 2560-2575 (2016).

- 637 9. Salomé, P., Weigel, D. & McClung, C. The role of the Arabidopsis morning loop
638 components CCA1, LHY, PRR7, and PRR9 in temperature compensation. *Plant Cell*
639 **22**, 3650-3661 (2010).
- 640 10. Edwards, K.D., Lynn, J.R., Gyula, P., Nagy, F. & Millar, A.J. Natural allelic variation
641 in the temperature-compensation mechanisms of the *Arabidopsis thaliana* circadian
642 clock. *Genetics* **170**, 387-400 (2005).
- 643 11. Edwards, K.D. *et al.* FLOWERING LOCUS C mediates natural variation in the high-
644 temperature response of the Arabidopsis circadian clock. *Plant Cell* **18**, 639 - 650
645 (2006).
- 646 12. Ito, S. *et al.* FLOWERING BHLH transcriptional activators control expression of the
647 photoperiodic flowering regulator *CONSTANS* in Arabidopsis. **109**, 3582-3587 (2012).
- 648 13. Gould, P.D. *et al.* Network balance via CRY signalling controls the Arabidopsis
649 circadian clock over ambient temperatures. **9**, 650 (2013).
- 650 14. Nagel, D.H., Pruneda-Paz, J.L. & Kay, S.A. FBH1 affects warm temperature responses
651 in the Arabidopsis circadian clock. **111**, 14595-14600 (2014).
- 652 15. Jones, M.A., Morohashi, K., Grotewold, E. & Harmer, S.L. Arabidopsis JMJD5/JMJ30
653 Acts Independently of LUX ARRHYTHMO Within the Plant Circadian Clock to
654 Enable Temperature Compensation. **10** (2019).
- 655 16. Gould, P.D. *et al.* The molecular basis of temperature compensation in the Arabidopsis
656 circadian clock. *Plant Cell* **18**, 1177-1187 (2006).
- 657 17. Doyle, M.R. *et al.* The ELF4 gene controls circadian rhythms and flowering time in
658 *Arabidopsis thaliana*. *Nature* **419**, 74-77 (2002).
- 659 18. Kolmos, E. *et al.* Integrating ELF4 into the circadian system through combined
660 structural and functional studies. *HFSP journal* **3**, 350-366 (2009).
- 661 19. Herrero, E. *et al.* EARLY FLOWERING4 recruitment of EARLY FLOWERING3 in
662 the nucleus sustains the Arabidopsis circadian clock. *Plant Cell* **24**, 428-443 (2012).
- 663 20. Nusinow, D.A. *et al.* The ELF4-ELF3-LUX complex links the circadian clock to
664 diurnal control of hypocotyl growth. *Nature* **475**, 398-402 (2011).
- 665 21. Khanna, R., Kikis, E.A. & Quail, P.H. EARLY FLOWERING 4 functions in
666 phytochrome B-regulated seedling de-etiolation. *Plant Physiol.* **133**, 1530-1538 (2003).
- 667 22. McWatters, H.G. *et al.* ELF4 is required for oscillatory properties of the circadian
668 clock. *Plant Physiol.* **144**, 391-401 (2007).
- 669 23. Helfer, A. *et al.* LUX ARRHYTHMO encodes a nighttime repressor of circadian gene
670 expression in the Arabidopsis core clock. *Curr. Biol.* **21**, 126-133 (2011).
- 671 24. Onai, K. & Ishiura, M. PHYTOCLOCK 1 encoding a novel GARP protein essential for
672 the Arabidopsis circadian clock. *Genes Cells* **10**, 963-972 (2005).
- 673 25. Hazen, S.P. *et al.* LUX ARRHYTHMO encodes a Myb domain protein essential for
674 circadian rhythms. *Proc. Natl. Acad. Sci. USA* **102**, 10387-10392 (2005).
- 675 26. Hicks, K.A. *et al.* Conditional circadian dysfunction of the *Arabidopsis early-flowering*
676 *3* mutant. *Science* **274**, 790-792 (1996).
- 677 27. Huang, H. *et al.* Identification of Evening Complex associated proteins in Arabidopsis
678 by affinity purification and mass spectrometry. *M. Cell. Proteomics* **15**, 201-217 (2016).
- 679 28. Li, G. *et al.* Coordinated transcriptional regulation underlying the circadian clock in
680 Arabidopsis. *Nat. Cell Biol.* **13**, 616-622 (2011).
- 681 29. Mizuno, T. *et al.* Ambient temperature signal feeds into the circadian clock
682 transcriptional circuitry through the EC night-time repressor in Arabidopsis thaliana.
683 *Plant Cell Physiol.* **55**, 958-976 (2014).
- 684 30. Siddiqui, H., Khan, S., Rhodes, B.M. & Devlin, P.F. FHY3 and FAR1 act downstream
685 of light stable phytochromes. *Front Plant Sci.* **7**, 175 (2016).
- 686 31. Ezer, D. *et al.* The evening complex coordinates environmental and endogenous signals
687 in Arabidopsis. *Nat. Plants* **3**, 17087 (2017).
- 688 32. Kim, Y. *et al.* ELF4 Regulates GIGANTEA Chromatin Access through Subnuclear
689 Sequestration. *Cell Reports* **3**, 671-677 (2013).

- 690 33. Nieto, C., López-Salmerón, V., Davière, J.-M. & Prat, S. ELF3-PIF4 Interaction
691 Regulates Plant Growth Independently of the Evening Complex. *Current Biology* **25**,
692 187-193 (2015).
- 693 34. Sai, J. & Johnson, C.H. Different circadian oscillators control Ca²⁺ fluxes and *lhcb*
694 gene expression. *Proc. Natl. Acad. Sci. USA* **96**, 11659-11663 (1999).
- 695 35. Thain, S.C., Murtas, G., Lynn, J.R., McGrath, R.B. & Millar, A.J. The circadian clock
696 that controls gene expression in Arabidopsis is tissue specific. *Plant Physiol.* **130**, 102-
697 110 (2002).
- 698 36. Michael, T.P., Salome, P.A. & McClung, C.R. Two Arabidopsis circadian oscillators
699 can be distinguished by differential temperature sensitivity. *Proc. Natl. Acad. Sci. USA*
700 **100**, 6878-6883 (2003).
- 701 37. Bordage, S., Sullivan, S., Laird, J., Millar, A.J. & Nimmo, H.G. Organ specificity in the
702 plant circadian system is explained by different light inputs to the shoot and root clocks.
703 *New Phytol.* **212**, 136-149 (2016).
- 704 38. Muranaka, T. & Oyama, T. Heterogeneity of cellular circadian clocks in intact plants
705 and its correction under light-dark cycles. *Sci. Adv.* **2**, e1600500 (2016).
- 706 39. Thain, S.C., Hall, A. & Millar, A.J. Functional independence of circadian clocks that
707 regulate plant gene expression. *Curr. Biol.* **10**, 951-956 (2000).
- 708 40. Fukuda, H., Nakamichi, N., Hisatsune, M., Murase, H. & Mizuno, T. Synchronization
709 of plant circadian oscillators with a phase delay effect of the vein network. *Phys. Rev.*
710 *Lett.* **99**, 098102 (2007).
- 711 41. Wenden, B., Toner, D.L.K., Hodge, S.K., Grima, R. & Millar, A.J. Spontaneous
712 spatiotemporal waves of gene expression from biological clocks in the leaf. *Proc. Natl.*
713 *Acad. Sci.* **109**, 6757-6762 (2012).
- 714 42. Greenwood, M., Domijan, M., Gould, P.D., Hall, A.J.W. & Locke, J.C.W. Coordinated
715 circadian timing through the integration of local inputs in Arabidopsis thaliana. *PLOS*
716 *Biology* **17**, e3000407 (2019).
- 717 43. Endo, M., Shimizu, H., Nohales, M.A., Araki, T. & Kay, S.A. Tissue-specific clocks in
718 Arabidopsis show asymmetric coupling. *Nature* **515**, 419-422 (2014).
- 719 44. Yakir, E. *et al.* Cell autonomous and cell-type specific circadian rhythms in
720 Arabidopsis. *Plant J.* **68** 520-531 (2011).
- 721 45. Gould, P.D. *et al.* Coordination of robust single cell rhythms in the Arabidopsis
722 circadian clock via spatial waves of gene expression. *Elife* **7**, e31700 (2018).
- 723 46. Fukuda, H., Ukai, K. & Oyama, T. Self-arrangement of cellular circadian rhythms
724 through phase-resetting in plant roots. *Phys. Rev. E.* **86**, 041917 (2012).
- 725 47. Takahashi, N., Hirata, Y., Aihara, K. & Mas, P. A hierarchical multi-oscillator network
726 orchestrates the Arabidopsis circadian system. *Cell* **163**, 148-159 (2015).
- 727 48. James, A.B. *et al.* The circadian clock in Arabidopsis roots is a simplified slave version
728 of the clock in shoots. *Science* **322**, 1832-1835 (2008).
- 729 49. Nimmo, H.G. Entrainment of Arabidopsis roots to the light:dark cycle by light pinging.
730 *Plant Cell Environ.* **41**, 1742-1748 (2018).
- 731 50. de Montaigu, A., Tóth, R. & Coupland, G. Plant development goes like clockwork.
732 *Trends in Genetics* **26**, 296-306 (2010).
- 733 51. Kolmos, E. *et al.* A Reduced-Function Allele Reveals That EARLY FLOWERING3
734 Repressive Action on the Circadian Clock Is Modulated by Phytochrome Signals in
735 Arabidopsis. *The Plant Cell* (2011).
- 736 52. Dixon, L.E. *et al.* Temporal Repression of Core Circadian Genes Is Mediated through
737 EARLY FLOWERING 3 in Arabidopsis. *Curr. Biol.* **21**, 120-125 (2011).
- 738 53. Kikis, E., Khanna, R. & Quail, P. ELF4 is a phytochrome-regulated component of a
739 negative feedback loop involving the central oscillator components CCA1 and LHY.
740 *Plant Journal* **44**, 300-313 (2005).
- 741 54. Lu, S.X. *et al.* CCA1 and ELF3 Interact in the Control of Hypocotyl Length and
742 Flowering Time in Arabidopsis. **158**, 1079-1088 (2012).
- 743 55. Huang, H. & Nusinow, D.A. Into the Evening: Complex Interactions in the Arabidopsis
744 Circadian Clock. *Trends in Genetics* **32**, 674-686 (2016).

- 745 56. Corbesier, L. *et al.* FT Protein Movement Contributes to Long-Distance Signaling in
746 Floral Induction of Arabidopsis. **316**, 1030-1033 (2007).
- 747 57. Jaeger, K.E. & Wigge, P.A. FT Protein Acts as a Long-Range Signal in Arabidopsis.
748 *Current Biology* **17**, 1050-1054 (2007).
- 749 58. Mathieu, J., Warthmann, N., Küttner, F. & Schmid, M. Export of FT Protein from
750 Phloem Companion Cells Is Sufficient for Floral Induction in Arabidopsis. *Current*
751 *Biology* **17**, 1055-1060 (2007).
- 752 59. Chen, X. *et al.* Shoot-to-Root Mobile Transcription Factor HY5 Coordinates Plant
753 Carbon and Nitrogen Acquisition. *Current Biology* **26**, 640-646 (2016).
- 754 60. Flis, A. *et al.* Defining the robust behaviour of the plant clock gene circuit with absolute
755 RNA timeseries and open infrastructure. *Open Biol* **5** (2015).
- 756 61. Salomé, P.A. & McClung, C.R. PSEUDO-RESPONSE REGULATOR 7 and 9 are
757 partially redundant genes essential for the temperature responsiveness of the
758 *Arabidopsis* circadian clock. *Plant Cell* **17**, 791-803 (2005).
- 759 62. Edwards, K.D. *et al.* Quantitative analysis of regulatory flexibility under changing
760 environmental conditions. *Mol. Syst. Biol.* **6** (2010).
- 761 63. Nakagawa, T. *et al.* Development of series of gateway binary vectors, pGWBs, for
762 realizing efficient construction of fusion genes for plant transformation. *J. Biosci.*
763 *Bioeng* **104**, 34-41 (2007).
- 764 64. Nakagawa, T. *et al.* Improved gateway binary vectors: high-performance vectors for
765 creation of fusion constructs in transgenic analysis of plants. *Biosci Biotechnol*
766 *Biochem.* **71**, 2095-2100 (2007).
- 767 65. Clough, S.J. & Bent, A.F. Floral dip: a simplified method for *Agrobacterium*-mediated
768 transformation of *Arabidopsis thaliana*. *Plant J.* **16**, 735-743 (1998).
- 769 66. Plautz, J.D. *et al.* Quantitative analysis of *Drosophila* period gene transcription in living
770 animals. *J. Biol. Rhythms* **12**, 204-217 (1997).
- 771 67. Czechowski, T., Stitt, M., Altmann, T., Udvardi, M.K. & Scheible, W.-R. Genome-
772 Wide Identification and Testing of Superior Reference Genes for Transcript
773 Normalization in Arabidopsis. *Plant Physiology* **139**, 5-17 (2005).
- 774 68. Dobin, A. *et al.* STAR: ultrafast universal RNA-seq aligner. *Bioinformatics* **29**, 15-21
775 (2013).
- 776 69. Liao, Y., Smyth, G.K. & Shi, W. featureCounts: an efficient general purpose program
777 for assigning sequence reads to genomic features. *Bioinformatics* **30**, 923-930 (2014).
- 778 70. Robinson, M.D., McCarthy, D.J. & Smyth, G.K. edgeR: a Bioconductor package for
779 differential expression analysis of digital gene expression data. *Bioinformatics* **26**, 139-
780 140 (2010).
- 781 71. Love, M.I., Huber, W. & Anders, S.J.G.B. Moderated estimation of fold change and
782 dispersion for RNA-seq data with DESeq2. *Genome Biol.* **15**, 550 (2014).
- 783 72. Tarazona, S., Garcia-Alcalde, F., Dopazo, J., Ferrer, A. & Conesa, A. Differential
784 expression in RNA-seq: A matter of depth. *Genome Res.* **21**, 2213-2223 (2011).
- 785 73. Leng, N. *et al.* EBSeq: an empirical Bayes hierarchical model for inference in RNA-seq
786 experiments. *Bioinformatics* **29**, 1035-1043 (2013).
- 787 74. Robinson, J.T. *et al.* Integrative genomics viewer. *Nat. Biotech.* **29**, 24-26 (2011).
- 788 75. Thorvaldsdóttir, H., Robinson, J.T. & Mesirov, J.P. Integrative Genomics Viewer
789 (IGV): high-performance genomics data visualization and exploration. *Brief. Bioinform.*
790 **14**, 178-192 (2013).
- 791 76. Michael, T.P. *et al.* Network discovery pipeline elucidates conserved time-of-day-
792 specific cis-regulatory modules. *PLoS Genetics* **4**, e14 (2008).
- 793 77. Mockler, T. *et al.* The DIURNAL project: DIURNAL and circadian expression
794 profiling, model-based pattern matching, and promoter analysis. *Cold Spring Harb.*
795 *Symp. Quant. Biol.* **72**, 353-363 (2007).
- 796 78. Katari, M.S. *et al.* VirtualPlant: A software platform to support systems biology
797 research. *Plant Physiol.* **152**, 500-515 (2010).
- 798 79. Takens, F. Detecting strange attractors in turbulence. *Lecture Notes in Math* **898**, 366-
799 381 (1981).

- 800 80. Stark, J. Delay embeddings for forced systems I. Deterministic forcing. *J. Nonlinear*
801 *Sci.* **9**, 255-332 (1999).
- 802 81. Marwan, N., Romano, C.M., Thiel, M. & Kurths, J. Recurrence plots for the analysis of
803 complex systems. *Phys. Rep.* **438**, 237-329 (2007).
- 804 82. Hirata, Y., Horai, S. & Aihara, K. Reproduction of distance matrices and original time
805 series from recurrence plots and their applications. *Eur. Phys. J. Spec. Top.* **164**, 13-22
806 (2008).
- 807 83. Tanio, M., Hirata, Y. & Suzuki, H. Reconstruction of driving forces through recurrence
808 plots. *Phys. Lett. A* **373**, 2031-2040 (2009).
- 809 84. Hirata, Y., Komuro, M., Horai, S. & Aihara, K. Faithfulness of Recurrence Plots: A
810 Mathematical Proof. *International Journal of Bifurcation and Chaos* **25**, 1550168
811 (2015).
- 812 85. Khor, A. & Small, M. Examining k-nearest neighbour networks: Superfamily
813 phenomena and inversion. *Chaos (Woodbury, N.Y.)* **26**, 043101-043101 (2016).
- 814 86. Small, M. *Applied Nonlinear Time Series Analysis: Applications in Physics, Physiology*
815 *and Finance.* (World Scientific, 2005).

816

817 **Acknowledgments**

818 We thank members of the Mas laboratory for helpful discussion and suggestions. We also thank
819 Prof. T. Nakagawa (Shimane University) and Meiji Seika Kaisha, Ltd. for the Gateway vectors.
820 We thank J. E. Salazar-Henao for tips on the Western-blot protocol in roots and Dr. I. Rubio-
821 Somoza for sharing the GFP antibody. Research in Y.H. laboratory is supported by JSPS
822 KAKENHI (Grant Number JP18K11461). S.J.D laboratory is funded by the Biotechnology and
823 Biological Sciences Research Council (BB/N018540/1). S.A.K. acknowledges support from the
824 National Institute of Health (GM067837). The Mas laboratory is funded from the
825 FEDER/Spanish Ministry of Economy and Competitiveness, from the Ramon Areces
826 Foundation and from the Generalitat de Catalunya (AGAUR). P.M. laboratory also
827 acknowledges financial support from the CERCA Program/Generalitat de Catalunya and by the
828 Spanish Ministry of Economy and Competitiveness through the “Severo Ochoa Program for
829 Centers of Excellence in R&D” 2016–2019 (SEV-2015-0533). W.W.C. is a recipient of a CSC
830 (Chinese Scholarship Council) fellowship.

831 **Author Contributions**

832 W.W.C, N.T. and J.R. performed the biological experiments. Y.H. performed the mathematical
833 analysis. S.P., S.J.D., D.A.N. and S.A.K. contributed with reagents and comments. P.M.
834 designed the experiments and wrote the manuscript. All authors read, revised, and approved the
835 manuscript.

836 **Competing interests**

837 The authors declare no competing interests.

838 **Additional information**

839 Extended data is available for this paper at XXX.

840 Supplementary information is available for this paper at XXX.

841 **Figure Legends**

842

843 **Fig. 1. Prevalent function of ELF4 sustaining circadian rhythms in roots.** **a**, Luminescence
844 of *CCA1::LUC* (*LUCIFERASE*) oscillation simultaneously measured in shoots (Sh)
845 (n=9) and roots (Rt) (n=9). Root luminescence signals are represented in the right Y-axis. **b**,
846 Period (left Y-axis) estimates of *CCA1::LUC* rhythms in shoots and roots (n=8 for each)
847 and amplitude (right Y-axis) estimates of *CCA1::LUC* rhythms in shoots (n=7) and
848 roots (n=8); data are represented as the median \pm max and min; 25-75 percentile). *** p-
849 value<0.0001; two-tailed t-tests with 95% of confidence. **c**, Circadian time course
850 analyses of *CCA1* mRNA expression in WT Sh and Rt. **d**, Luminescence of
851 *CCA1::LUC* rhythms in WT (n=9) and *elf4-1* Rt (n=8). **e**, Luminescence of *LHY::LUC*
852 rhythms in WT (n=8) and ELF4-ox Rt (n=9). **f**, Circadian time course analyses of *PRR9*
853 mRNA expression in roots of WT and *elf4-1*. Sampling was performed under constant
854 light conditions (LL) following synchronization under light:dark cycles (LD). **a, c-f**,
855 Data are represented as the means + SEM. **g**, Heatmap of the median-normalized expression (Z-
856 scaled FPKM values) of DEGs following a hierarchical clustering using the Euclidean
857 distance. **h**, Relationship between average expression and fold change for each gene. **i**,
858 Volcano plot showing fold-change versus significance of the differential expression test.
859 Black dots represent genes that are not differentially expressed, while red and green dots
860 are the genes that are significantly up- and down-regulated, respectively. Circadian
861 phases of **j**, up- and **k**, down-regulated DEG in *elf4-1* roots. Radial axis represents the
862 subjective time (hours). White and gray areas represent subjective day and night,
863 respectively. The “n” values refer to independent samples. **a-k**, Data for all experiments
864 are representative of two biological replicates, with measurements taken from distinct
865 samples grown and processed at different times.

866

867 **Fig. 2. ELF4 moves from shoots to regulate rhythms in roots.** *CCA1::LUC* luminescence in
868 roots of ELF4-ox scion into **a**, *elf4-1* (n=4) and **b**, *elf4-2* (n=3) rootstocks. Water instead of
869 luciferin was added to the wells containing ELF4-ox shoots. *CCA1::LUC* luminescence in *elf4-*
870 *1* rootstocks with **c**, WT (n=8) and **d**, ELF4 Minigene (ELF4MG) (n=10) scions. WT scions do
871 not express reporters and water instead of luciferin was added to the wells containing ELF4MG
872 shoots. **a-d**, Schematic drawings depicting the different scion/rootstock combinations are shown
873 above each graph. **e**, Circadian time course analyses of *ELF4* mRNA expression in roots of WT,
874 *elf4-1* and ELF4-ox scion and *elf4-1* rootstocks. **f**, Luminescence of *LHY::LUC* rhythms in *elf4-*

875 *I* roots after injection in shoots of purified ELF4 (n=4) or GFP proteins (n=8) and *elf4-1* roots
876 as a control (n=6). **g**, Representative image showing the lack of fluorescence signals in roots of
877 WT scion and WT rootstock. **h**, Representative image showing fluorescence signals in roots of
878 ELF4-ox scion into *elf4-1* rootstock. Scale bar: 100 μ m. **i**, Western-blot analysis of ELF4-GFP
879 protein accumulation (arrows) in roots of ELF4-ox-GFP scion (E4ox) grafted into *elf4-1*
880 rootstock (*e4-1*) (two pools of independent grafting assays, #1 and #2, are shown). Asterisks
881 denote non-specific bands. **j**, *CCA1::LUC* luminescence in *elf4-2* rootstocks grafted with
882 ELF4-x3GFP scions (n=5). Water instead of luciferin was added to the wells containing ELF4-
883 x3GFP shoots. **a-f, j**, Data are represented as the means + SEM. **k**, Protein features of various
884 plant mobile proteins. The “n” values refer to independent samples. **a-j**, Two biological
885 replicates were performed for all experiments, with measurements taken from distinct samples
886 grown and processed at different times.
887

888 **Fig. 3. Mobile ELF4 does not regulate the photoperiodic-dependent phase in roots.**
889 Luminescence analyses of *PRR9::LUC* rhythms in **a**, roots (n=5 for ShD, n=6 for LgD) and **b**,
890 shoots (n=6 for ShD, n=4 for LgD) of plants grown under short day (ShD) or long day (LgD)
891 conditions. **c**, Western-blot analyses and **d**, quantification of ELF4 protein accumulation in
892 ELF4 Minigene roots (E4MG Rt) of plants grown under ShD and LgD (also in Extended Data
893 Fig. 8a-d). **e**, Western-blot analyses and **f**, quantification of ELF4 protein accumulation in
894 E4MG roots of plants grown under ShD and excised roots under LgD (also in Extended Data
895 Fig. 8a-f). Arrows indicate the ELF4 protein. Luminescence of *LHY::LUC* oscillation in WT,
896 ELF4-ox and *elf4-1* plants measured in **g**, shoots (Sh) (n=12) and **h**, roots (Rt) (n=12) under
897 LgD conditions. **a-b, d, f, g-h**, Data are represented as the means + SEM. Dashed lines indicate
898 dusk under LgD. The “n” values refer to independent samples. **a-h**, Two biological replicates
899 were performed for all experiments, with measurements taken from distinct samples grown and
900 processed at different times.
901

902 **Fig. 4. Mobile ELF4 sets the temperature-dependent pace of the root clock.**

903 Individual luminescence waveforms of *CCA1::LUC* rhythmic oscillation in ELF4-ox scion into
904 *elf4-1* rootstocks at **a**, 12°C (n=10) and **b**, 28°C (n=8). Individual luminescence waveforms of
905 *CCA1::LUC* rhythmic oscillation in E4MG scion into *elf4-1* rootstocks at **c**, 12°C (n=7) and **d**,
906 28°C (n=8). Water instead of luciferin was added to the wells containing ELF4-ox and E4MG
907 scions. **e**, Luminescence of *LHY::LUC* rhythmic oscillation in WT and ELF4-ox roots at 28°C
908 (n=8 for WT, n=5 for ELF4-ox). Data are represented as the means + SEM. **f**, Western-blot
909 analysis of ELF4-GFP protein accumulation (arrow) in roots of ELF4-ox-GFP scion (E4ox)
910 grafted into *elf4-1* rootstock (*e4-1*) at 12°C and 28°C. *elf4-1* mutant protein extracts were used

911 as a control. Asterisks denote non-specific bands. Ponceau S staining of the membrane is shown
912 in the right panel. Schematic drawing depicting **g**, the increased shoot-to-root movement of
913 ELF4 (Sh-to-Rt mov, thick blue vertical arrows), increased *PRR9* repression and the slow pace
914 of the root clock at low temperatures, and **h**, the decreased shoot-to-root movement (Sh-to-Rt
915 mov, thin red vertical arrows), decreased *PRR9* repression and fast-paced root clock at high
916 temperature. The “n” values refer to independent samples. **a-f**, Two biological replicates were
917 performed for all experiments, with measurements taken from distinct samples grown and
918 processed at different times.

Figure 1

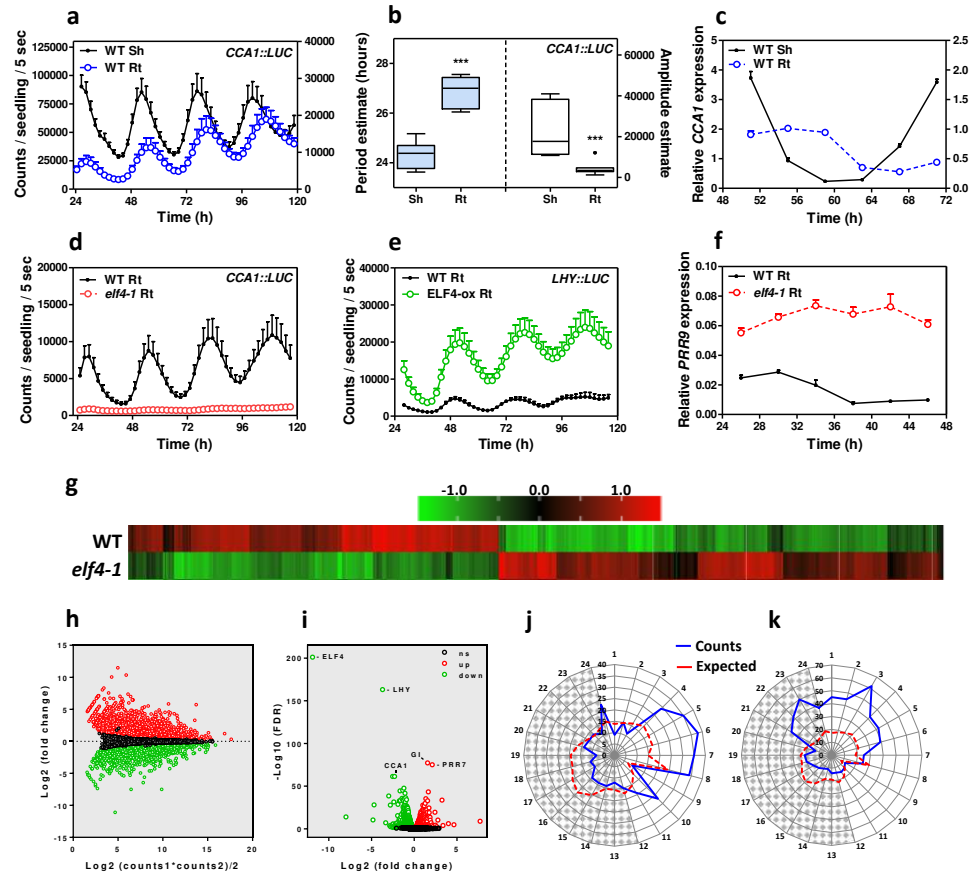


Figure 2

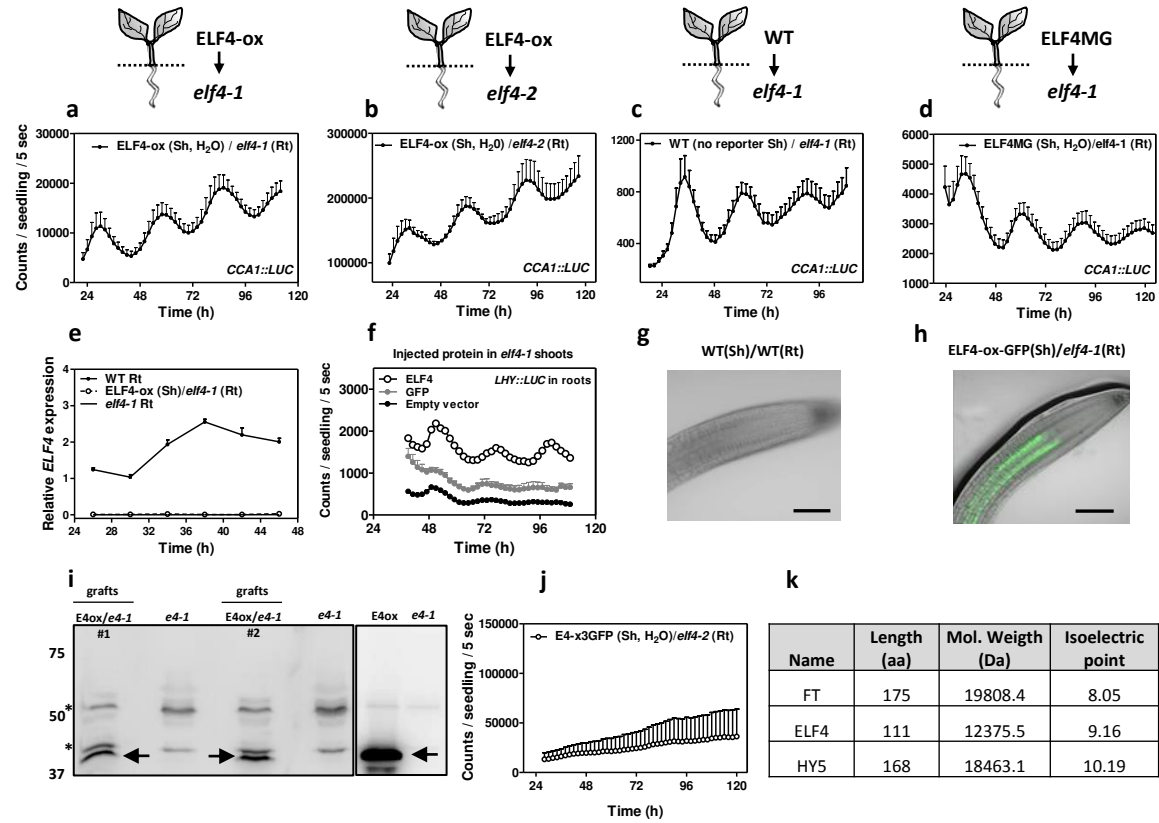
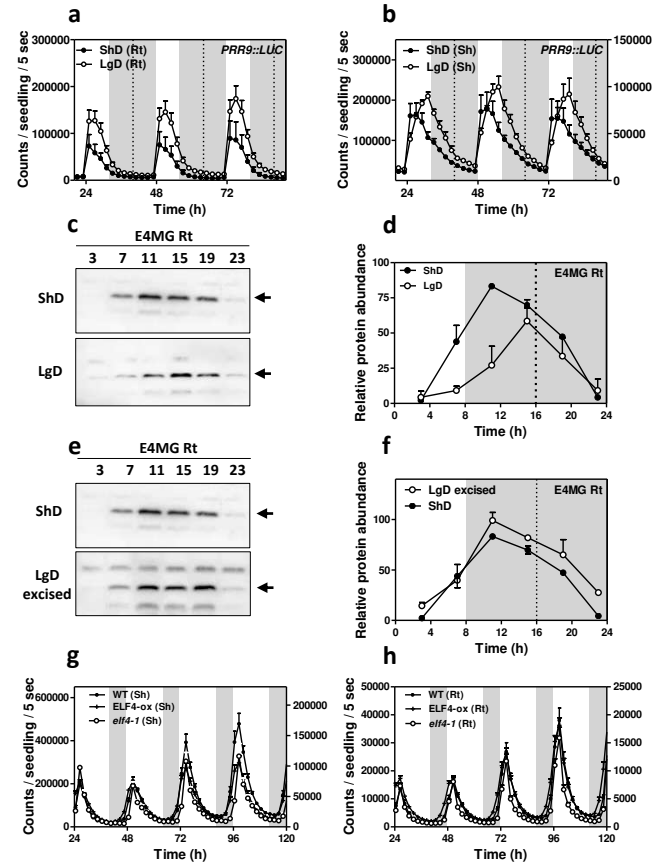
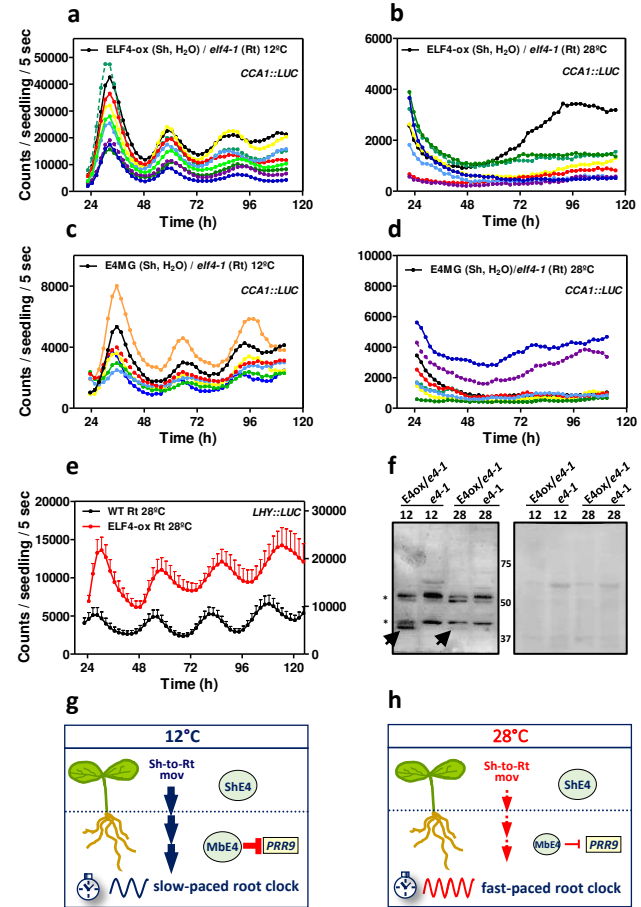
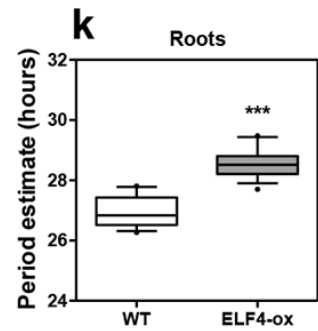
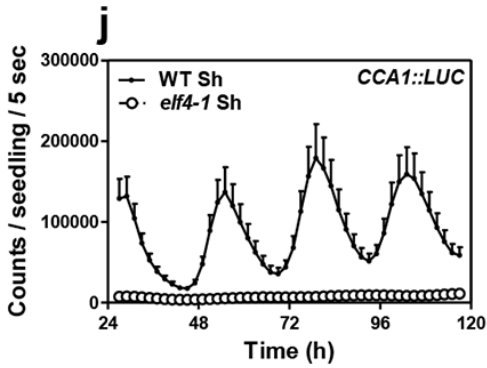
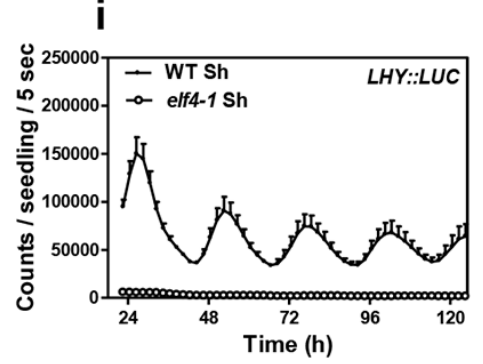
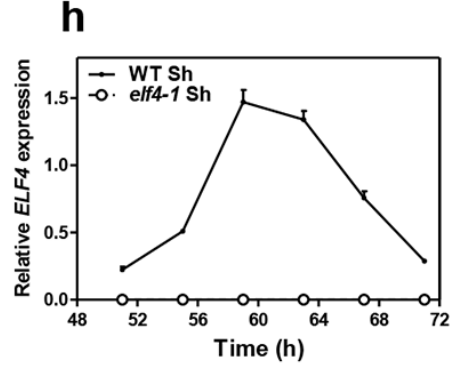
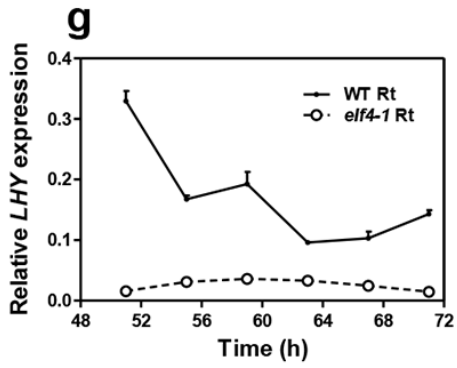
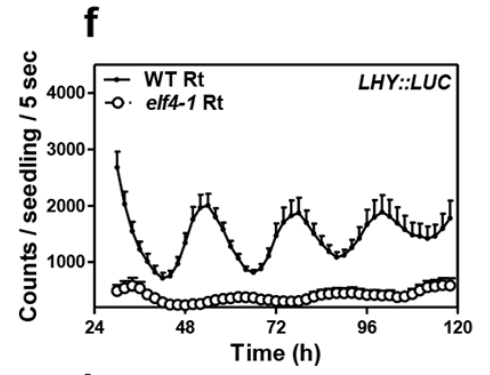
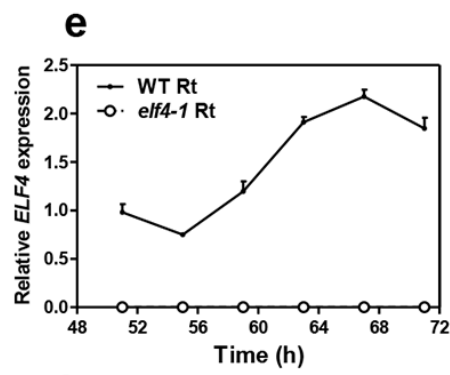
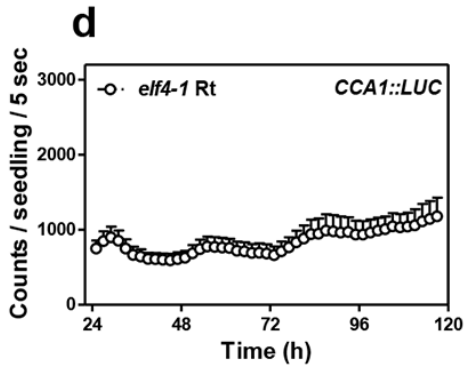
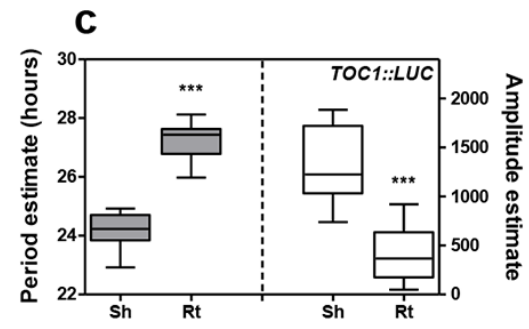
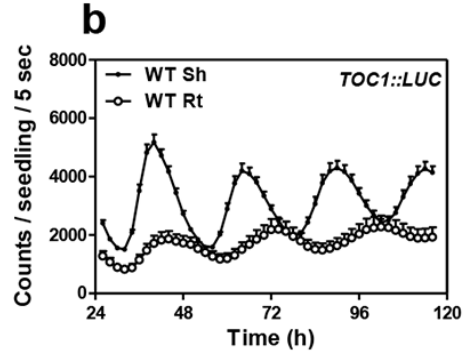
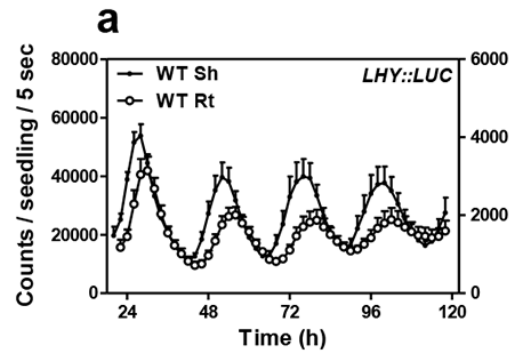
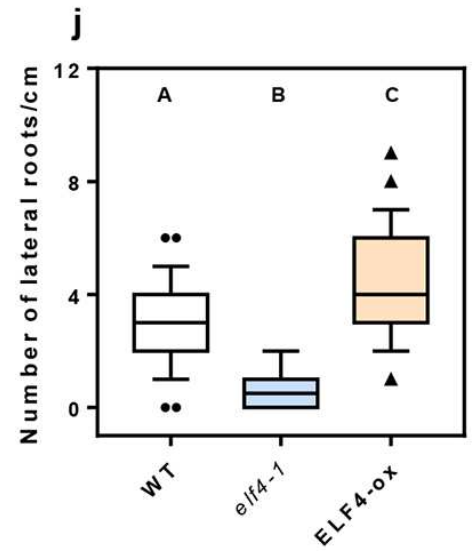
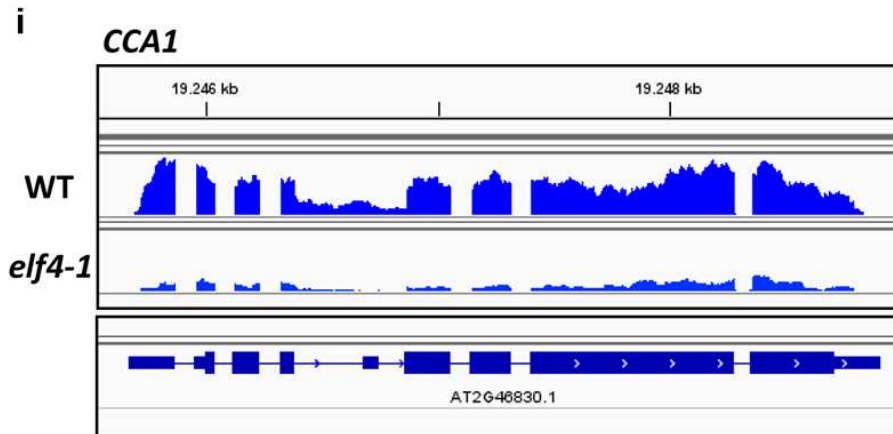
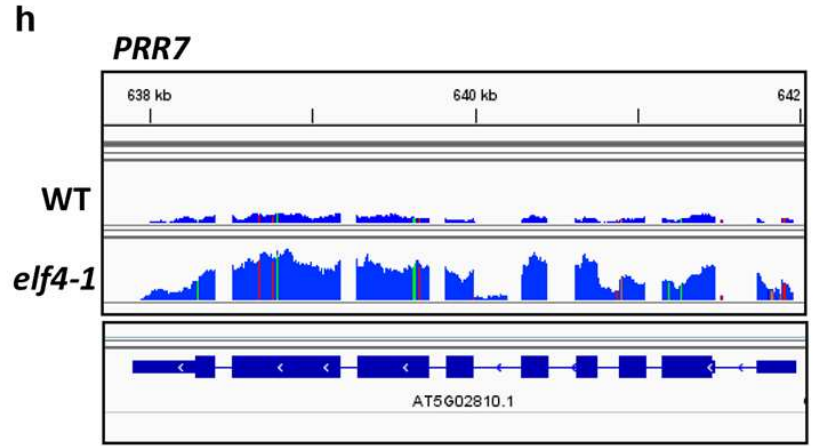
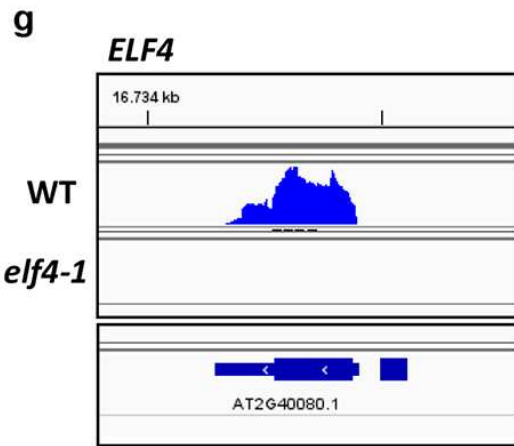
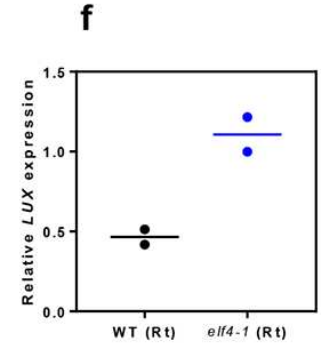
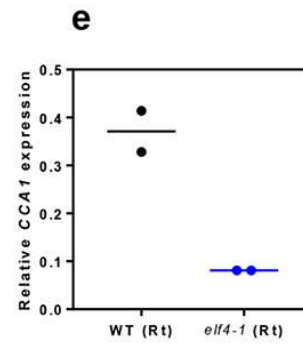
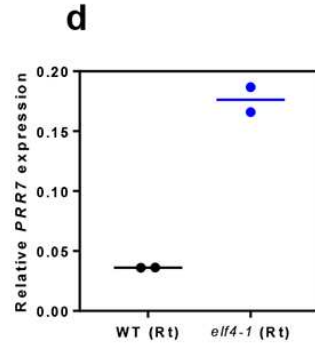
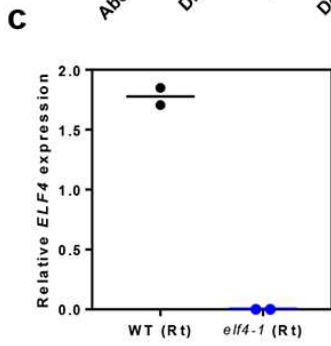
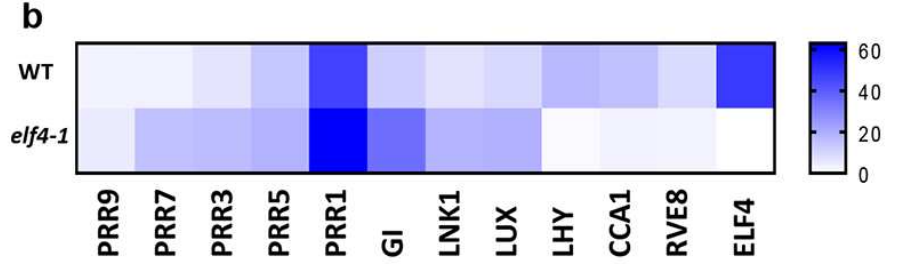
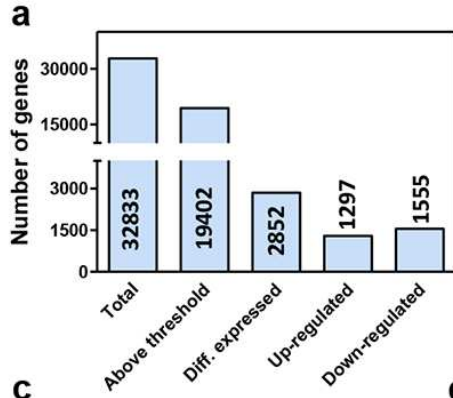


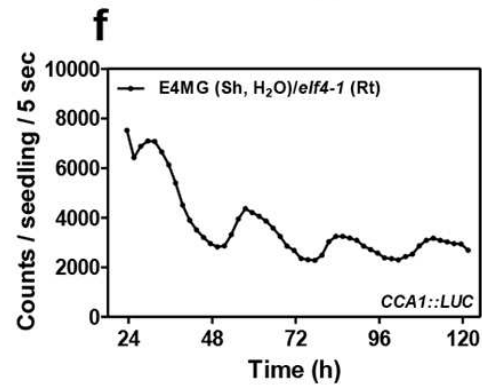
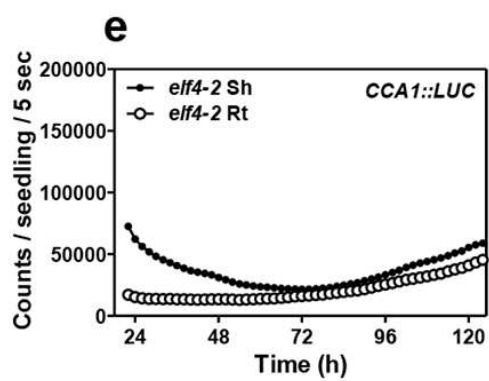
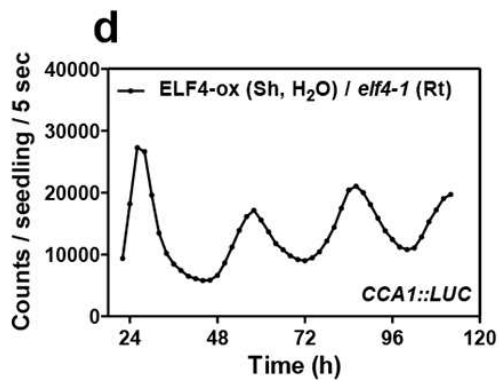
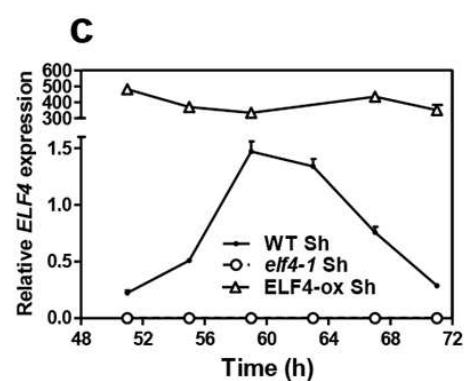
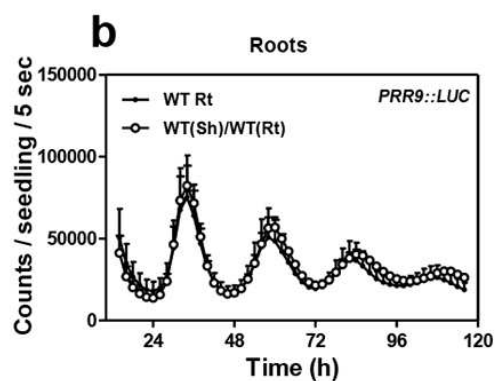
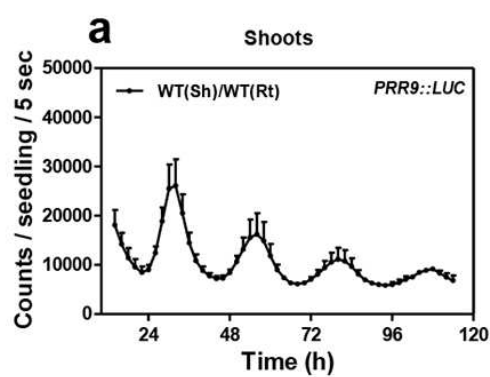
Figure 3

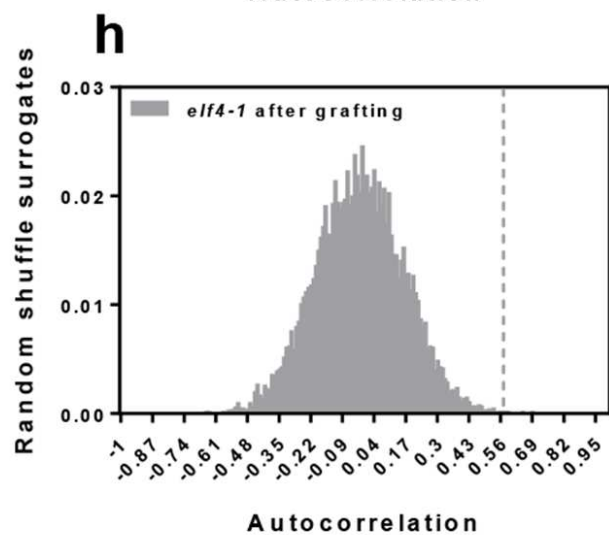
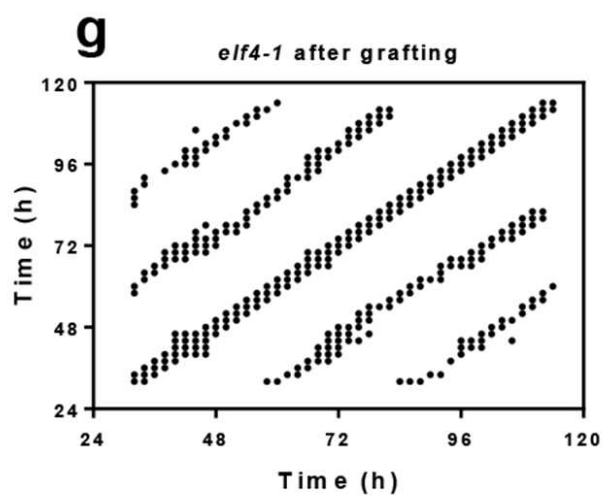
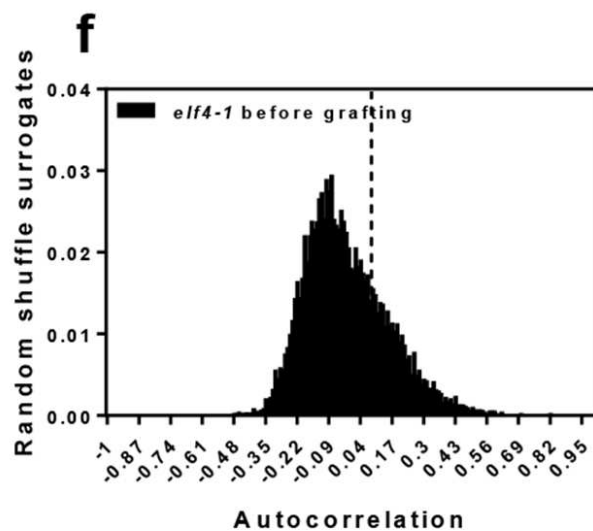
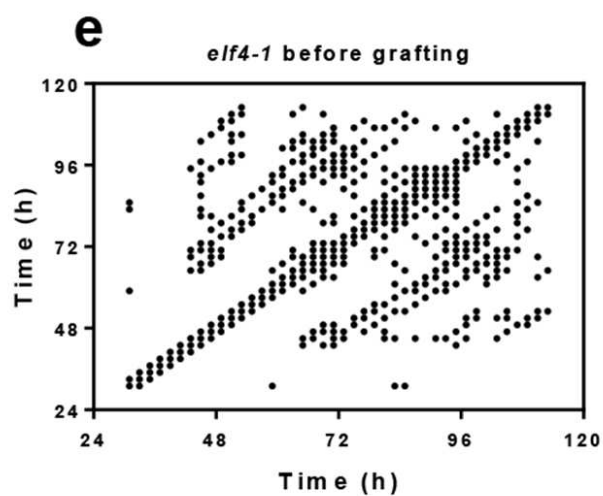
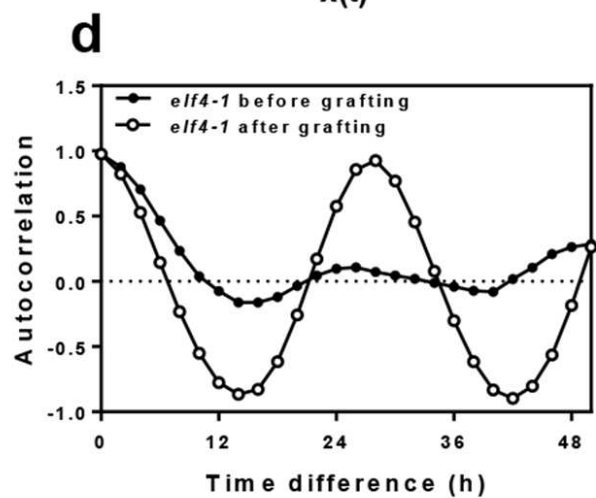
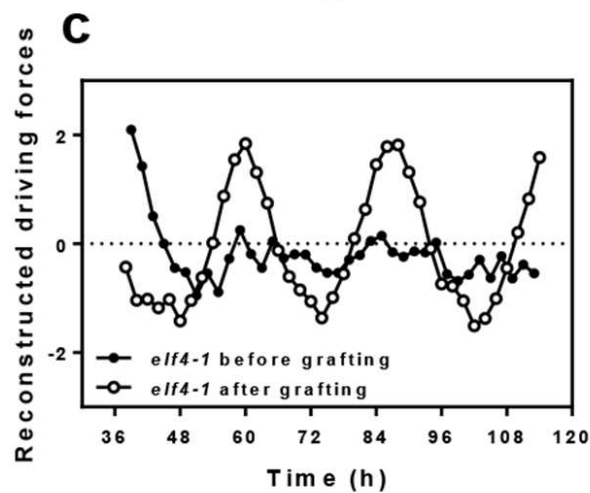
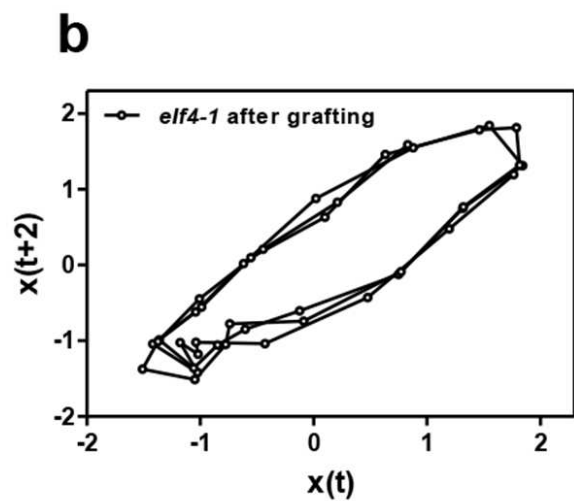
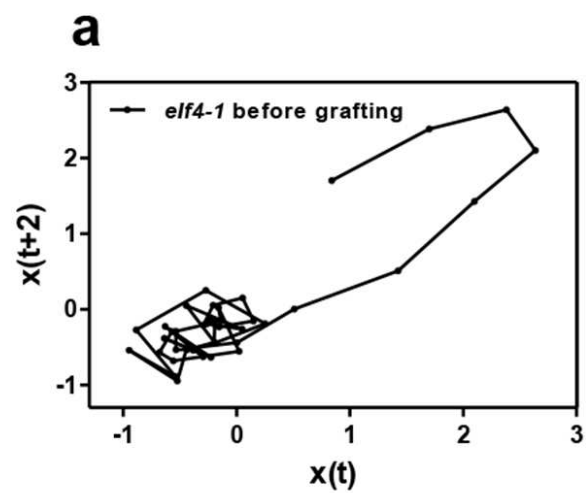


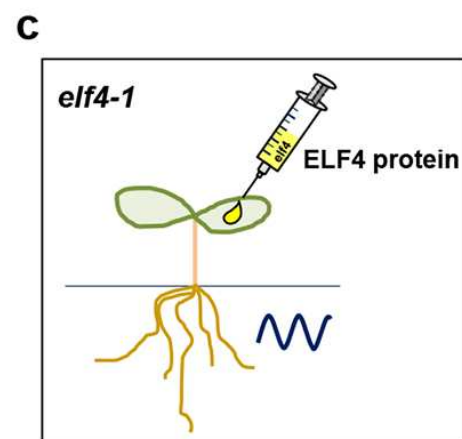
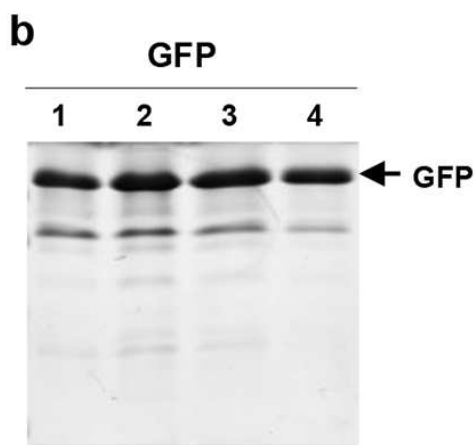
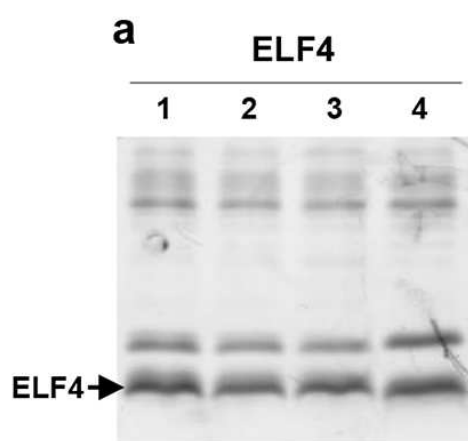




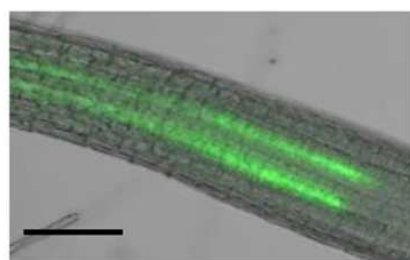




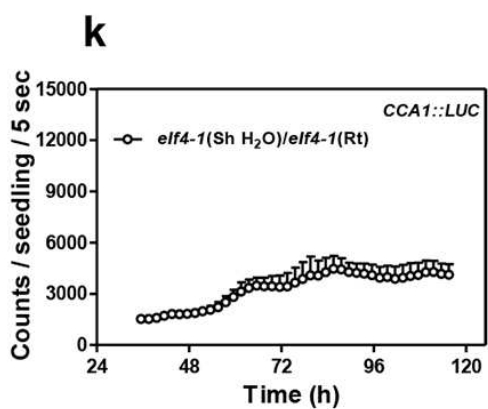
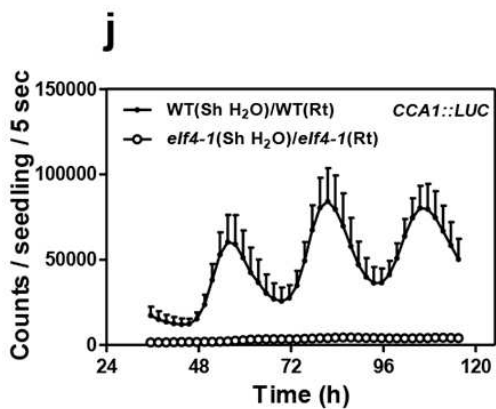
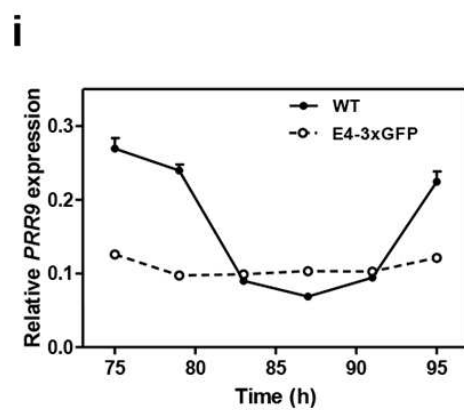
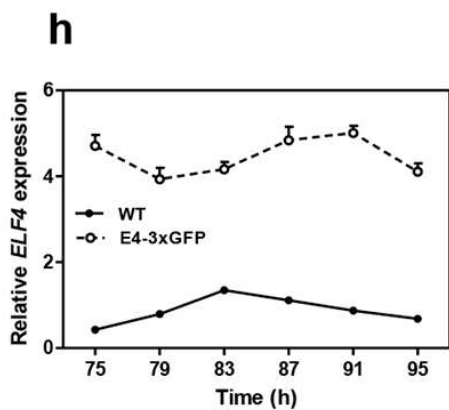
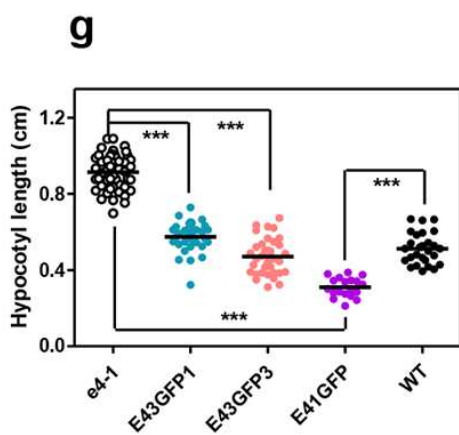
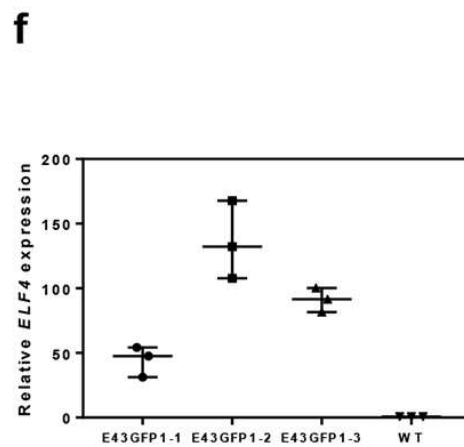
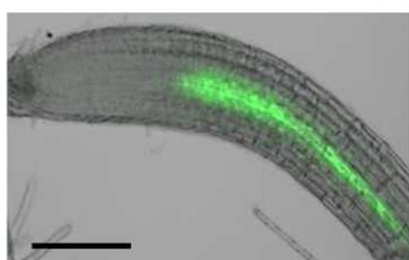


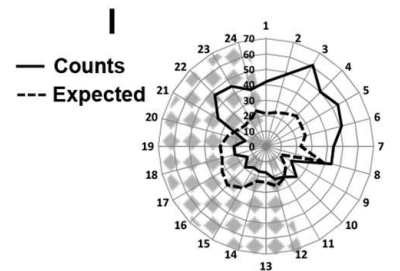
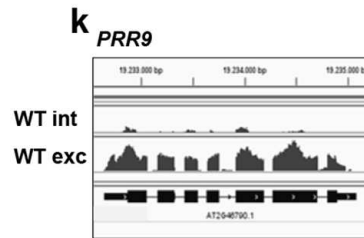
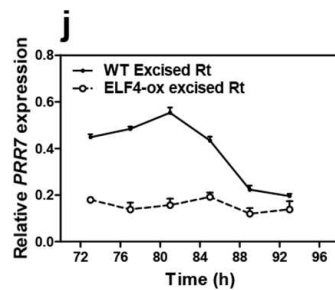
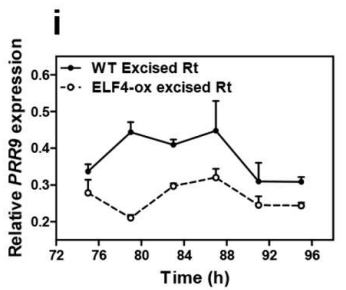
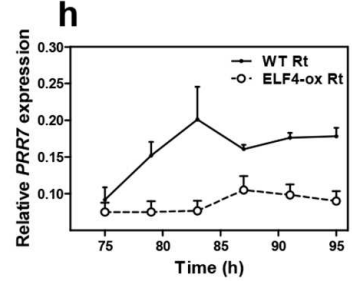
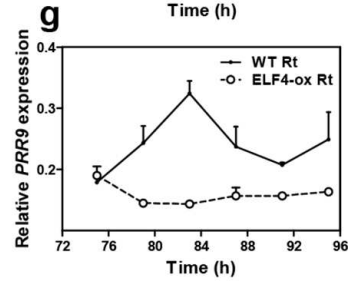
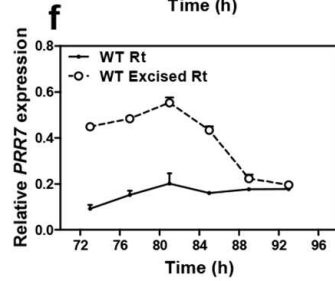
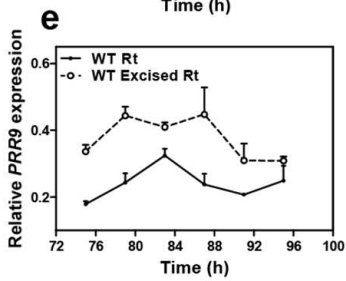
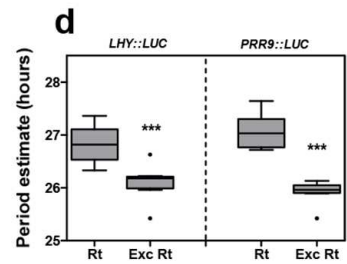
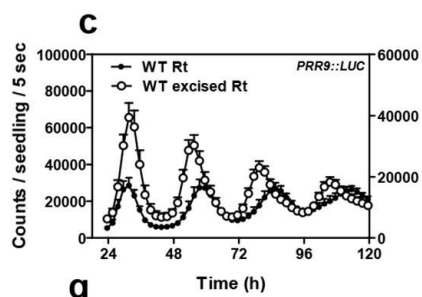
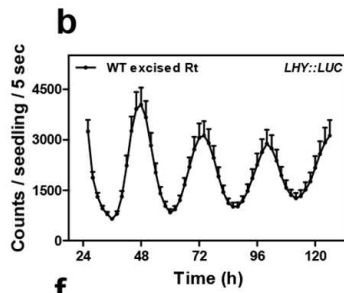
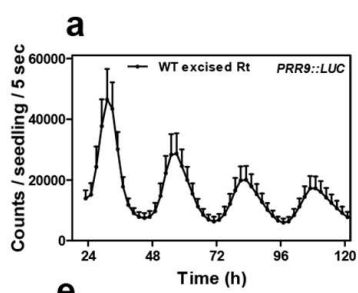


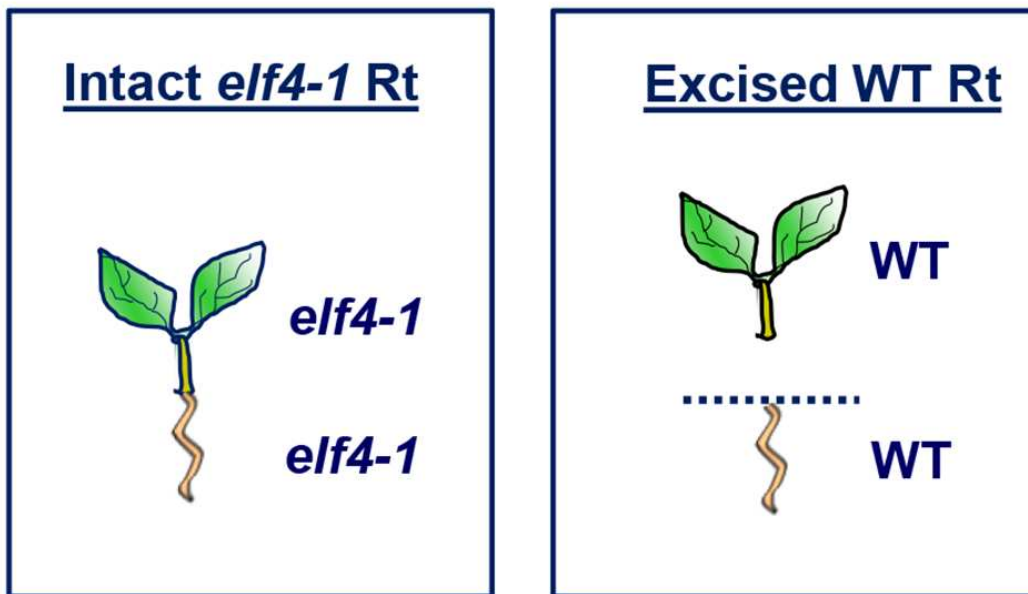
d **ELF4-ox-GFP(Sh)/*elf4-1*(Rt)**



e **ELF4-ox-GFP(Sh)/*elf4-1*(Rt)**

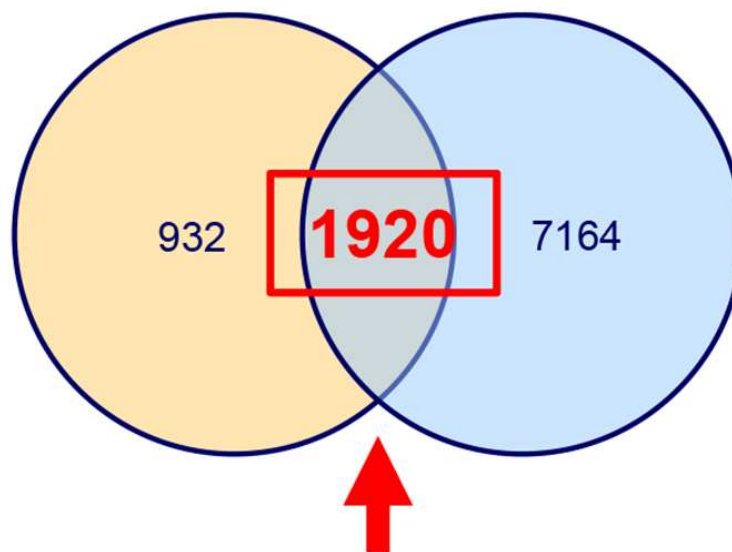






elf4-1 intact

WT excised



67,32% of the DEGs in *elf4-1* intact roots are also differentially regulated in WT excised roots. The overlapped DEGs are not affected by excision as *elf4-1* mutant roots are intact.

